

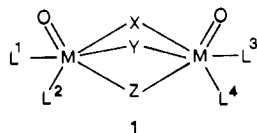
Triply Bridged Binuclear Complexes of the (Organodiazenido)molybdenum and the (Organodiazenido)rhenium Cores. Crystal and Molecular Structures of $[\text{HNEt}_3]_2[\text{Mo}_2(\text{NNPh})(\text{NNHPh})(\text{SCH}_2\text{CH}_2\text{S})_3(\text{SCH}_2\text{CH}_2\text{SH})] \cdot 2/3\text{H}_2\text{NNHPh}$, $[\text{HNEt}_3][\text{Mo}_2(\text{NNPh})_4(\text{SPh})_5]$, and $[\text{HNEt}_3][\text{Re}_2(\text{NNPh})_2(\text{SPh})_7]$

Tze-Chen Hsieh, Terrence Nicholson, and Jon Zubieta*

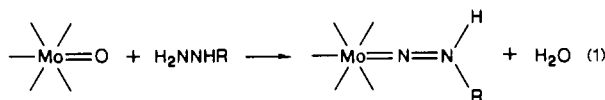
Received October 15, 1986

Reactions of $[\text{MoO}_2(2,3\text{-butanediolate})_2] \cdot 2(\text{butane-2,3-diol})$ with phenylhydrazine in methanol, followed by an arenethiolate ligand, yield complex binuclear anions with (organodiazenido)molybdenum centers triply bridged by thiolato groups. The synthesis of analogous rhenium species may be accomplished from appropriate precursors and the properties compared to those of the molybdenum complexes. The chemical and structural consequences of the thiolate ligand type are illustrated by the structures of $[\text{Mo}_2(\text{NNHPh})(\text{NNPh})(\text{SCH}_2\text{CH}_2\text{S})_3(\text{SCH}_2\text{CH}_2\text{SH})]^{2-}$ (2^{2-}) and $[\text{Mo}_2(\text{NNPh})_4(\text{SPh})_5]^-$ ($3a^-$), isolated as $[\text{HNEt}_3]^+$ salts. Complex **2** exhibits gross geometric features common to the triply bridged class of molybdenum-oxo and tungsten-oxo species. Each molybdenum center is coordinated to the sulfur donors of a terminal bidentate ethanedithiolate ligand, three bridging thiolate donors from a bidentate bridging dimercaptoethane group and a monodentate dithiolate, and the α -nitrogen of a linearly coordinated organodiazenido (NNR) or organohydrazido(2-) (NNHR) ligand. The short Mo–Mo distance of 2.837 Å is consistent with the metal–metal interaction invoked for this type of complex; similar structural details are observed for the structure of $[\text{HNEt}_3][\text{Re}_2(\text{NNPh})_2(\text{SPh})_7]$ (**4**), synthesized from the reaction of $[\text{ReCl}(\text{NNPh})_2(\text{PPh}_3)_2]$ with thiophenol. In contrast, complex **3a**, while exhibiting the triply thiolate-bridged geometry, presents a Mo–Mo distance of 3.527 (1) Å and bridge symmetry consistent with the description of the structure in terms of confacial octahedra, rather than edge-sharing square pyramids with a long axially bridging interaction, the appropriate description for all other members of this class of triply bridged binuclear complexes. Crystal data: for **2**, triclinic space group $P1$, $a = 10.224$ (2) Å, $b = 10.874$ (3) Å, $c = 35.942$ (8) Å, $\alpha = 86.59$ (1)°, $\beta = 88.79$ (1)°, $\gamma = 61.96$ (1)°, $V = 3520.5$ (10) Å³, $Z = 3$, and $R = 0.052$ for 5699 reflections; for **3a**, triclinic space group $P1$, $a = 10.994$ (2) Å, $b = 12.173$ (2) Å, $c = 24.179$ (4) Å, $\alpha = 91.03$ (1)°, $\beta = 91.45$ (1)°, $\gamma = 109.78$ (1)°, $V = 3042.9$ (12) Å³, $Z = 2$, and $R = 0.059$ for 4763 reflections; for **4**, monoclinic space group $P2_1/n$, $a = 16.137$ (2) Å, $b = 9.863$ (2) Å, $c = 16.668$ (2) Å, $\beta = 111.12$ (1)°, $V = 2474.4$ (7) Å³, $Z = 4$, and $R = 0.055$ for 2984 reflections.

Although a number of triply bridged binuclear oxo-molybdenum^{1–8} and oxotungsten^{9–11} complexes of type **1** are



known, examples of triply bridged binuclear species with cores other than the metal–oxo moiety are relatively rare.¹² The organodiazenido–metal core, $[\text{M}(\text{NNR})]^{n+}$, is a robust functional unit, synthetically accessible via a simple condensation reaction, eq 1, presumably followed by some internal redox step, perhaps



- Buchanan, I.; Clegg, W.; Garner, C. D.; Sheldrick, G. M. *Inorg. Chem.* **1983**, *22*, 3657.
- Huneke, J. T.; Yamanouchi, K.; Enemark, J. H. *Inorg. Chem.* **1978**, *17*, 3695.
- Gelder, J. I.; Enemark, J. H.; Wolterman, G.; Boston, D. A.; Haight, G. P. *J. Am. Chem. Soc.* **1975**, *97*, 1616.
- Dance, I. G.; Landers, A. E. *Inorg. Chem.* **1979**, *18*, 3487.
- Yamanouchi, K.; Enemark, J. H.; McDonald, J. W.; Newton, W. E. *J. Am. Chem. Soc.* **1977**, *99*, 3529.
- Bunzey, G.; Enemark, J. H.; Gelder, J. I.; Yamanouchi, K.; Newton, W. E. *J. Less-Common Met.* **1977**, *54*, 101.
- Boyd, I. W.; Dance, I. G.; Landers, A. E.; Wedd, A. G. *Inorg. Chem.* **1979**, *18*, 1875.
- Dilworth, J. R.; Neaves, B. D.; Dahlstrom, P.; Hyde, J.; Zubieta, J. *Transition Met. Chem. (Weinheim, Ger.)* **1982**, *7*, 257.
- Hanson, G. R.; Brunnetti, A. A.; McDonell, A. C.; Murray, K. S.; Wedd, A. G. *J. Am. Chem. Soc.* **1981**, *103*, 1953. Bradbury, J. R.; Masters, A. F.; McDonell, A. C.; Brunnetti, A. A.; Bond, A. M.; Wedd, A. G. *J. Am. Chem. Soc.* **1981**, *103*, 1959.
- Patel, V. D.; Boorman, P. M.; Kerr, K. A.; Moynihan, K. J. *Inorg. Chem.* **1982**, *21*, 1385.
- Ball, J. M.; Boorman, P. M.; Moynihan, K. J.; Richardson, J. R. *Acta Crystallogr., Sect. C: Cryst. Struct. Commun.* **1985**, *C41*, 47.
- Blower, P. J.; Dilworth, J. R.; Hutchinson, J. P.; Zubieta, J. A. *J. Chem. Soc., Dalton Trans.* **1985**, 1533.

involving M–OH, to remove the remaining hydrogen atom. The core appears capable of stabilizing the triply bridging geometry.^{13–15} Furthermore, metal–diazenido and metal–hydrazido complexes are of intrinsic interest as potential intermediates in the abiological reduction of dinitrogen to ammonia and have been extensively investigated as probes for the properties of sulfur-ligated metals.^{16,17}

- Hsieh, T.-C.; Gebreyes, K.; Zubieta, J. *J. Chem. Soc., Chem. Commun.* **1984**, 1172.
- Nicholson, T.; Zubieta, J. *Inorg. Chim. Acta* **1985**, *100*, L35.
- Hsieh, T.-C.; Zubieta, J. *Inorg. Chim. Acta* **1985**, *99*, L47.
- Chatt, J.; Pearman, A. J.; Richards, R. L. *J. Chem. Soc., Dalton Trans.* **1977**, 2139. Bossard, G. E.; George, T. A.; Howell, D. B.; Koczon, L. M.; Lester, R. K. *Inorg. Chem.* **1983**, *22*, 1968.
- Dilworth, J. R.; Zubieta, J. A. *J. Chem. Soc., Chem. Commun.* **1981**, 132.
- Knobler, C.; Penfold, B. R.; Robinson, W. T.; Wilkins, C. J.; Yong, S. H. *J. Chem. Soc., Dalton Trans.* **1980**, 248. Butcher, R. J.; Penfold, B. R.; Sinn, E. *J. Chem. Soc., Dalton Trans.* **1979**, 688.
- Carillo, D.; Gouzerh, P.; Jeannin, Y. *Nouv. J. Chim.* **1985**, *9*, 749.
- Hsieh, T.-C.; Zubieta, J. *Polyhedron* **1986**, *5*, 305. Hsieh, T.-C.; Zubieta, J. *Inorg. Chem.* **1985**, *24*, 1287.
- Blower, P. J.; Dilworth, J. R.; Hutchinson, J.; Nicholson, T.; Zubieta, J. *J. Chem. Soc., Dalton Trans.* **1985**, 2639.
- Dilworth, J. R.; Harrison, S. A.; Walton, D. R. M.; Schweda, E. *Inorg. Chem.* **1985**, *24*, 1287.
- Boyd, I. W.; Dance, I. G.; Murray, K. S.; Wedd, A. G. *Aust. J. Chem.* **1978**, *31*, 279.
- Dance, I. G.; Wedd, A. G.; Boyd, I. W. *Aust. J. Chem.* **1978**, *31*, 519.
- Burt, R. J.; Dilworth, J. R.; Leigh, G. J.; Zubieta, J. *J. Chem. Soc., Dalton Trans.* **1982**, 2295.
- Bruce, A.; Corbin, J. L.; Dahlstrom, F. L.; Hyde, J. R.; Minelli, M.; Stiefel, E. I.; Spencer, J. T.; Zubieta, J. A. *Inorg. Chem.* **1986**, *25*, 917.
- Chatt, J.; Crichton, B. A. L.; Dilworth, J. R.; Dahlstrom, P.; Gutkoske, R.; Zubieta, J. *Inorg. Chem.* **1982**, *21*, 2385.
- Dilworth, J. R.; Zubieta, J.; Hyde, J. R. *J. Am. Chem. Soc.* **1982**, *104*, 365.
- Hillhouse, G. K.; Haymore, B. L.; Bistram, S. A.; Hermann, W. G. *Inorg. Chem.* **1983**, *22*, 314.

We have recently demonstrated the ability of thiolate ligands to stabilize triply bridged binuclear complexes incorporating a variety of metal-diazenido cores.¹³⁻¹⁵ In this paper, we present the full details of the synthesis and structural characterizations of the complexes $[\text{HNEt}_3][\text{Mo}_2(\text{NNPh})(\text{NNHPh})(\text{SCH}_2\text{CH}_2\text{S})_3(\text{SCH}_2\text{CH}_2\text{SH})]^{2-}/_3\text{H}_2\text{NNHPh}$ (**2**), $[\text{HNEt}_3][\text{Mo}_2(\text{NNPh})_4(\text{SPh})_3]$ (**3**), and $[\text{HNEt}_3][\text{Re}_2(\text{NNPh})_2(\text{SPh})_7]$ (**4**). Complex **3** represents a rare example of the bis(diazenido)molybdenum core, $[\text{Mo}(\text{NNR})_2]^{n+}$, and a unique example of a triply bridged binuclear species with no direct metal-metal interaction. This observation demonstrates a remarkable flexibility of the triply bridged core in accommodating metal-metal distances in a range of 2.63–3.53 Å.

Experimental Section

Materials and Methods. All preparative reactions were performed in freshly distilled, dry solvents, and unless otherwise noted, no special precautions to eliminate atmospheric oxygen were taken. Reagent grade solvents were used throughout. All other reagents were obtained from standard commercial sources and used without further purification.

The following instruments were used in this work: IR, Perkin-Elmer 283B infrared spectrophotometer; UV/visible, Varian DMSO 90 UV/visible spectrophotometer; X-ray crystallography, Nicolet R3m automated diffractometer; electrochemistry, BAS100 electroanalytical system.

All compounds were isolated as crystalline solids. Microanalytical data were obtained by MicAnal, Tucson, Arizona.

Synthesis of $[\text{HNEt}_3]_2[\text{Mo}_2(\text{NNPh})(\text{NNHPh})(\text{SC}_2\text{H}_4\text{S})_3(\text{SC}_2\text{H}_4\text{SH})]^{2-}/_3\text{H}_2\text{NNHPh}$ (2**).** Method I: from $[\text{Mo}(\text{NNPh})_2(\text{C}_4\text{H}_9\text{O}_2)_2] \cdot 2\text{C}_2\text{H}_5\text{O}_2$. Reaction of $[\text{MoO}_2(\text{bd})_2] \cdot 2\text{H}_2\text{bd}$ ³² (1 g, 2.0 mmol) (bd = butane-2,3-diolate) with excess phenylhydrazine (2 mL, 20.0 mmol) in 40 mL of methanol, after being refluxed for 6 h, gave the complex $[\text{Mo}(\text{NNPh})_2(\text{bd})_2] \cdot \text{H}_2\text{NNHPh}$ (1.02 g, 86%) as a bright red powder. Anal. Calcd for $\text{C}_{26}\text{H}_{38}\text{MoN}_6\text{O}_4$: C, 52.5; H, 6.39; N, 14.2. Found: C, 51.7; H, 6.32; N, 13.9.

$[\text{HNEt}_3]_2[\text{Mo}_2(\text{NNPh})(\text{NNHPh})(\text{SC}_2\text{H}_4\text{S})_3(\text{SC}_2\text{H}_4\text{SH})]^{2-}/_3\text{H}_2\text{NNHPh}$ was prepared from a solution of $[\text{Mo}(\text{NNPh})_2(\text{bd})_2] \cdot \text{H}_2\text{NNHPh}$ (3.0 g, 5.0 mmol) in a mixture of 10 mL of NEt_3 and 50 mL of methanol at 70 °C to which $\text{HSC}_2\text{H}_4\text{SH}$ (5 mL, 60.0 mmol) was added slowly with stirring. After being refluxed for 4 h, this solution was cooled to room temperature and filtered and diethyl ether was layered carefully over the solution. After this mixture was allowed to stand for several weeks at room temperature, dark purple crystals were observed to be growing at the solvent interface. Yield: 1.52 g (58% based on Mo). Anal. Calcd for $\text{C}_{35}\text{H}_{65}\text{Mo}_2\text{N}_7\text{S}_8$: C, 40.8; H, 6.31; N, 9.51. Found: C, 40.2; H, 6.25; N, 9.21.

Method II: from $[\text{HNEt}_3]_2[\text{Mo}_4\text{O}_8(\text{OMe})_2(\text{NNPh})_4]$. $[\text{HNEt}_3]_2[\text{Mo}_4\text{O}_8(\text{OMe})_2(\text{NNPh})_4]$ ³³ (2 g, 1.67 mmol) and thiophenol (2 mL, 19.5 mmol) were added to 50 mL of methanol. After being refluxed for 4 h, the solution, whose color changed from red to black, was allowed to cool to room temperature, and diethyl ether was layered carefully over the solution. After this mixture was allowed to stand for 1 week at 0 °C, black crystals were observed to be growing at the solvent interface. Yield: 1.62 g (38.5% based on Mo). Anal. Calcd for $\text{C}_{60}\text{H}_{61}\text{Mo}_2\text{N}_9\text{S}_5$: C, 57.2; H, 4.85; N, 10.01. Found: C, 56.4; H, 4.76; N, 9.82.

Synthesis of $[\text{HNEt}_3][\text{Mo}_2(\text{NNPh})_4(\text{SPh})_3]$ (3a**).** Complexes of the type $[\text{HNEt}_3][\text{Mo}_2(\text{NNPh})_4(\text{SAR})_3]$ were synthesized in a manner analogous to that used to synthesize $[\text{HNEt}_3]_2[\text{Mo}_2(\text{NNPh})(\text{NNHPh})(\text{SC}_2\text{H}_4\text{S})_3(\text{SC}_2\text{H}_4\text{SH})]^{2-}/_3\text{H}_2\text{NNHPh}$ by using the appropriate substituted thiophenol instead of 1,2-dimercaptoethane. Details of the reactions with thiophenol are presented. The complexes $[\text{HNEt}_3][\text{Mo}_2(\text{NNPh})_4(\text{SC}_6\text{H}_4\text{X})_3]$ (X = 4-Me, **3b**; X = 4-Cl, **3c**; X = OCH₃, **3d**) were synthesized by analogous preparative routes.

Method I. Reaction of $[\text{Mo}(\text{NNPh})_2(\text{bd})_2] \cdot \text{H}_2\text{NNHPh}$ (3.0 g, 5.0 mmol) with excess thiophenol (6.2 mL, 60 mmol) in a mixture of 10 mL of NEt_3 and 50 mL of methanol, after being refluxed for 4 h, gave

complex **3a** in 40% yield (2.3 g) as a black precipitate. Recrystallization from $\text{CH}_2\text{Cl}_2/\text{hexane}$ or $\text{CS}_2/\text{hexane}$ gave lustrous purple-black crystals in 20% overall yield. Anal. Calcd for $\text{C}_{60}\text{H}_{61}\text{Mo}_2\text{N}_9\text{S}_5$: C, 57.2; H, 4.85; N, 10.01. Found: C, 56.8; H, 4.79; N, 9.87.

Method II. $[\text{HNEt}_3]_2[\text{Mo}_4\text{O}_8(\text{OCH}_3)_2(\text{NNPh})_4]$ (2 g, 1.67 mmol) and $\text{HSC}_2\text{H}_4\text{SH}$ (2 mL, 24.0 mmol) were added to 50 mL of methanol. After being refluxed for 4 h, the solution, whose color changed red to dark purple, was allowed to cool to room temperature, and diethyl ether was layered carefully over the solution. After this mixture was allowed to stand for 1 week at 0 °C, dark purple crystals were observed to be growing at the solvent interface. Yield: 2.18 g of (62.5% based on Mo). Anal. Calcd for $\text{C}_{35}\text{H}_{65}\text{Mo}_2\text{N}_7\text{S}_8$: C, 40.8; H, 6.31; N, 9.51. Found: C, 40.1; H, 6.21; N, 9.70.

Synthesis of $[\text{HNEt}_3][\text{Re}_2(\text{NNPh})_2(\text{SPh})_7]$ (4**).** Oxotrichlorobis(triphenylphosphine)rhenium (2.0 g), phenylhydrazine hydrochloride (1.75 g), and triethylamine (7.0 mL) were refluxed with stirring in 200 mL of dry methanol for 45 min. The solution turned from yellow to orange-brown with the formation of a maroon precipitate as heating proceeded. The precipitate $[\text{ReCl}(\text{PPh}_3)_2(\text{NNPh})_2]$ was collected, washed with methanol and air dried. Anal. Calcd for the *p*-bromophenyldiazenido derivative $[\text{ReCl}(\text{PPh}_3)_2(\text{NNC}_6\text{H}_4\text{Br}-4)_2]$, which was prepared analogously ($\text{C}_{48}\text{H}_{38}\text{N}_4\text{P}_2\text{ClBr}_2\text{Re}$): C, 51.6; H, 3.4; N, 5.1. Found: C, 50.8; H, 3.3; N, 5.4.

Chlorobis(triphenylphosphine)bis(phenyldiazenido)rhenium (0.5 g), thiophenol (0.5 mL), and triethylamine (5 mL) in 400 mL of benzene were warmed gently overnight with stirring under nitrogen. The resulting deep red solution was filtered and the solvents removed by rotary evaporation. The red oil was dissolved in dichloromethane and layered with anhydrous diethyl ether, from which small red crystals of $\text{Re}(\text{SPh})(\text{NNPh})_2(\text{PPh}_3)_2$ formed gradually. The mother liquor was again layered with anhydrous diethyl ether, giving dark filamentous crystals of **4** in 40% yield. Anal. Calcd for $\text{C}_{60}\text{H}_{61}\text{Re}_2\text{N}_9\text{S}_7$: C, 49.7; H, 4.21; N, 4.84. Found: C, 49.1; H, 4.03; N, 4.78.

X-ray Crystallography. The details of the crystal data, data collection methods, and refinement procedures are given in Table I. Full details of the crystallographic methodologies may be found in ref 26. Atomic positional parameters for the structures of **2**, **3a**, and **4** are given in Tables III–V, respectively.

In the case of compound **2**, peak search routines generated the space group *P1* with three dimeric units per cell or *P1* with three molybdenum centers per asymmetric unit. A check was made on the crystal symmetry by taking Weissenberg and precession photographs of three separate crystals mounted along different crystal axes. The lengths of the three triclinic axes were confirmed by these photographs and by exhaustive but unsuccessful searches for significant intensity at positions corresponding to half-integral values for one or more indices simultaneously. No equivalences of reflection intensities consistent with Laue symmetry other than triclinic were revealed in a careful study of the data. Whereas the data reduction for triclinic symmetry gave a merging *R* of 0.012, assumption of trigonal or hexagonal Laue symmetry gave merging *R* values in the range 0.250–0.350.

Although reflection statistics are heavily biased toward the acentric space group, attempts were made to solve the structure in the centric space group *P1̄*, assuming 1.5 molecules in the asymmetric unit. Such an assignment requires that one dimer unit be located at a center of symmetry, affording disordered ligand geometry about the Mo centers. Although the unique binuclear unit appeared to refine relatively smoothly, no adequate disorder model was produced. The refinement was deemed unsuccessful as the best disorder model afforded a residual of 0.20–0.25 with inconsistent bond lengths and temperature factors and large correlations. Refinement of the inverted structure in *P1* yielded no significant improvement in fit. The choice of space group appears to be correct. It may be noted that the analogous complex $[\text{NEt}_4][\text{Mo}_2\text{O}_2(o\text{-MeC}_6\text{H}_4\text{S})_6(\text{OMe})]$ also crystallizes in an acentric space group with three dimeric units per asymmetric unit.

Results and Discussion

Preparation and Characterization of the Complexes. We have examined the reactions of organodiazenido(2-) and organohydrazido(2-) complexes of rhenium and molybdenum with monodentate and bidentate thiolate ligands. The complex dioxobis(butanediolato(1-)) molybdenum(VI)—bis(butanediol), $[\text{MoO}_2(\text{Hbd})_2] \cdot 2\text{H}_2\text{bd}$,¹⁸ reacts with phenylhydrazine in methanol in an condensation-type reaction to yield a complex analyzing for $[\text{Mo}(\text{NNPh})_2(\text{Hbd})_2] \cdot \text{H}_2\text{NNHPh}$ but exhibiting spectroscopic properties similar to those of the recently characterized $[\text{Mo}_2(\text{NNPh})_4(\text{OMe})_2(\text{acac})_2]$,¹⁹ suggesting a dimeric or polynuclear formulation. The reactions of this material with thiolate ligands fall into three categories depending on the properties of the ligand.

- (30) Cotton, F. A.; Ucko, D. A. *Inorg. Chim. Acta* **1972**, *6*, 161.
 (31) Sutton, D. *Chem. Soc. Rev.* **1975**, *4*, 443. Avitable, G.; Ganis, P.; Nimiroff, M. *Acta Crystallogr., Sect. B: Struct. Crystallogr. Cryst. Chem.* **1971**, *B27*, 725. Duckworth, V. F.; Douglas, P. G.; Mason, R.; Shaw, B. L. *J. Chem. Soc., Chem. Commun.* **1970**, 1083. Carroll, W. E.; Lalor, F. J. *J. Chem. Soc., Dalton Trans.* **1973**, 1754. Ibers, J. A.; Haymore, B. L. *Inorg. Chem.* **1975**, *14*, 1369. McArdle, J. V.; Schultz, A. J.; Corbin, B. J.; Eisenbert, R. *Inorg. Chem.* **1973**, *12*, 1676. Cowie, M.; Haymore, B. L.; Ibers, J. A. *Inorg. Chem.* **1975**, *14*, 2617. Haymore, B. L.; Ibers, J. A. *Inorg. Chem.* **1975**, *14*, 1369.
 (32) Butcher, R. J.; Penfold, B. R. *J. Cryst. Mol. Struct.* **1976**, *6*, 1.
 (33) Hsieh, T.-C.; Zubieta, J. *Inorg. Chem.* **1985**, *24*, 1287.

Table I. Summary of Experimental Details for the Crystallographic Studies of $[\text{HNEt}_3]_2[\text{Mo}_2(\text{NNPh})(\text{NNHPh})(\text{SCH}_2\text{CH}_2\text{S})_3(\text{SCH}_2\text{CH}_2\text{SH})]^{2-} \cdot \frac{2}{3}\text{H}_2\text{NNHPh}$ (**2**), $[\text{HNEt}_3][\text{Mo}_2(\text{NNPh})_4(\text{SPh})_5]$ (**3a**), and $[\text{HNEt}_3][\text{Re}_2(\text{NNPh})_2(\text{SPh})_7]$ (**4**)

	2	3a	4
(A) Crystal Parameters at 23 °C ^a			
<i>a</i> , Å	10.224 (2)	10.994 (2)	10.951 (2)
<i>b</i> , Å	10.874 (3)	12.173 (2)	25.198 (4)
<i>c</i> , Å	35.942 (8)	24.179 (4)	24.112 (4)
α , deg	86.59 (1)	91.03 (1)	90.00
β , deg	88.79 (1)	91.45 (1)	100.32 (1)
γ , deg	61.96 (1)	109.78 (1)	90.00
<i>V</i> , Å ³	3520.5 (10)	3042.9 (12)	6545.9 (8)
space group	<i>P</i> 1	$P\bar{1}$	<i>P</i> 2 ₁ / <i>n</i>
<i>Z</i>	3	2	4
<i>D</i> _{calcd} , g cm ⁻³	1.48	1.38	1.47
(B) Measurement of Intensity Data			
cryst dims, mm	0.31 × 0.28 × 0.33	0.40 × 0.31 × 0.38	0.22 × 0.28 × 0.19
instrument	Nicolet R3m		
radiation	Mo K α ($\lambda = 0.71069$ Å)		
scan mode	coupled $\theta(\text{cryst})-2\theta(\text{counter})$		
scan rate, deg/min	7-30		
scan range, deg	2.0 < 2 θ ≤ 45		
scan length, deg	from [2 θ (K $\alpha_1 - 1.0$)] to [2 θ (K $\alpha_2 + 1.0$)]		
bkgd measmt	stationary cryst, stationary counter, at the beginning and end of each 2 θ scan, each for the time taken for the scan		
stds	3 collected every 197		
no. of reflns collected	6219	9238	6343
no. of indep reflns, $F_o \geq 6\sigma(F_o)$	5699	4763	2984
(C) Reduction of Intensity Data and Summary of Structure Solution and Refinement ^b			
Data Corrected for Background, Attenuators, and Lorentz and Polarization Effects in the Usual Fashion			
abs coeff	8.82 cm ⁻¹	6.10 cm ⁻¹	70.02
abs cor	not applied to 2 and 3 ; based on χ scans for 5 reflns with χ angles near 90° or 270° in the case of 4		
<i>T</i> _{max} / <i>T</i> _{min}	1.03	1.11	1.19
structure soln	Patterson synthesis yielded the metal positions; all remaining non-hydrogen atom located via standard Fourier techniques for all three structures		
atom scattering factors ^c	neutral atomic scattering factors were used throughout the analysis		
anomalous dispersion ^d	applied to all non-hydrogen atoms		
final discrepancy factor ^e			
<i>R</i>	0.052	0.055	0.055
<i>R</i> _w	0.061	0.059	0.055
goodness of fit ^f	1.494	1.587	1.353

^a From a least-squares fitting of the setting angle of 25 reflections. ^b All calculations were performed on a Data General Nova 3 computer with 32K of 16-bit words using local versions of the Nicolet SHELXTL interactive crystallographic software package as described in: Sheldrick, G. M. *Nicolet SHELXTL Operations Manual*; Nicolet XRD Corp.: Cupertino, CA, 1979. ^c Cromer, D. T.; Mann, J. B. *Acta Crystallogr., Sect. A: Cryst. Phys., Diffr. Theor. Gen. Crystallogr.* **1968**, *24*, 321. ^d *International Tables for X-ray Crystallography*; Kynoch: Birmingham, England, 1974; Vol. III. ^e $R = \sum [|F_o| - |F_c|] / \sum |F_o|$; $R_w = [\sum w(|F_o| - |F_c|)^2 / \sum w|F_o|^2]^{1/2}$; $w = 1/\sigma^2(F_o) + g^*(F_o)$; $g = 0.005$. ^f $\text{GOF} = [\sum w(|F_o| - |F_c|)^2 / (\text{NO} - \text{NV})]^{1/2}$ where NO is the number of observations and NV is the number of variables.

Table II. Electrochemical Parameters for the Triply Bridged Binuclear Complexes **2** and **3a**

complex	$E_{1/2}$ or E_p^{ox} , ^a V	E_p^{red} - E_p^{ox} , mV	$i_p^{\text{red}}/i_p^{\text{ox}}$	$i_p/Cv^{1/2,d}$ mA s ^{1/2} mV ^{-1/2} M ⁻¹	<i>e</i> / <i>M</i> ^e
2	+0.911	<i>c</i>		7.9	1.0
	-1.122	<i>c</i>		7.9	1.0
3	+1.167	<i>c</i>		11.9	<i>f</i>
	+0.696	70	1.4	8.2	1.0
	+0.552	73	1.6	8.2	1.0
	-1.459	<i>c</i>		8.1	1.0

^a At a platinum-bead working electrode, using solutions 1.0×10^{-3} M in complex in 0.1 M (*n*-Bu₄N)PF₆ in CH₂Cl₂. All potentials are referred to the ferrocene/ferrocenium couple. Cyclic voltammograms were obtained at a sweep rate of 200 mV s⁻¹. ^b Estimated from $E_{1/2}^{\text{ox}} = (E_p^{\text{ox}} - E_p^{\text{red}})/2 \sim E_p^{\text{ox}} - 29$ mV. The shape parameter $E_p^{\text{ox}} - E_{p/2}^{\text{ox}}$ lay within the range 60-80 mV for all complexes. ^c No reverse wave observed. ^d The current function for the ferrocene/ferrocenium couple at the same electrode is 8.5 mA s^{1/2} mV^{-1/2} M⁻¹. ^e The value of *e*/*M* was determined by controlled-potential electrolysis at a potential 0.2 V beyond the process of interest. ^f Multielectron process.

With ethanedithiol the dianionic, formally molybdenum(V) binuclear species $[\text{Mo}_2(\text{NNPh})(\text{NNHPh})(\text{SCH}_2\text{CH}_2\text{S})_3(\text{SCH}_2\text{CH}_2\text{SH})]^{2-}$ is isolated as the triethylammonium salt (**2**), while with arenethiolates (HSC₆H₄X, X = H, 4-Me, 4-Cl, 4-OMe) the anionic, formally molybdenum(0) (if one uses the diazeni-

do(+1) formalism for the -NNR ligand) binuclear complexes $[\text{Mo}_2(\text{NNPh})_4(\text{SC}_6\text{H}_4\text{X})_5]^-$ are isolated as the triethylammonium salts (**3a-d**). The empirical formulations for **2** and **3a-d** were based on microanalysis and integration of the NMR spectra. In addition, the diamagnetism of the complexes, as inferred from the sharp, unperturbed NMR spectra, is consistent with the binuclear formulation. The X-ray crystal structures of **2** and **3a** confirmed these assignments.

The infrared spectrum of the dark violet complex **2** shows bands at 1602 cm⁻¹ and 1568 cm⁻¹ characteristic of $\nu(\text{N}=\text{N})$ for coordinated diazenido and hydrazido groups, respectively. The electronic spectrum exhibits charge transfer bands at 210 and 272 nm with molar extinction coefficients of ca. 4×10^4 M⁻¹ cm⁻¹. The medium-intensity band at 544 nm ($\epsilon = 2 \times 10^3$ M⁻¹ cm⁻¹) may be associated with the [M(NNR)] chromophore.

The purple complex **3a** exhibits medium-intensity infrared bands at 1640 and 1611 cm⁻¹, characteristic of asymmetric and symmetric $\nu(\text{N}-\text{N})$ stretch for the *cis*-bis(diazenido) moiety. The medium-intensity transition at 524 nm in the electronic spectrum is associated with the [Mo(NNR)₂]²⁺ chromophore.²⁰

Reactions using the sterically demanding thiolate 2,4,6-triisopropylthiophenol, in acetonitrile yielded only the previously described mononuclear product $[\text{Mo}(\text{SAr})_3(\text{NNPh})(\text{CH}_3\text{CN})]$.²¹ The identity of this product was confirmed by X-ray photographs and unit cell dimensions.

Table III. Atom Coordinates ($\times 10^4$) and Temperature Factors ($\text{\AA}^2 \times 10^3$) for $[\text{HNEt}_3]_2[\text{Mo}_2(\text{NNPh})(\text{NNHPh})(\text{SCH}_2\text{CH}_2\text{S})(\text{SCH}_2\text{CH}_2\text{SH})]$ (2)

atom	x	y	z	$U_{\text{eq/iso}}^a$	atom	x	y	z	$U_{\text{eq/iso}}^a$
Mo(1)	10000	10000	10000	32 (1)*	S(6b)	7409 (4)	2349 (3)	6234 (1)	36 (2)*
Mo(2)	9575 (1)	525 (1)	9218 (1)	34 (1)*	S(7b)	9633 (4)	-591 (4)	6116 (1)	39 (2)*
S(1)	8449 (4)	1226 (4)	10534 (1)	44 (2)*	S(8b)	11185 (9)	-2982 (6)	5316 (2)	113 (4)*
S(2)	12015 (5)	-409 (4)	10441 (1)	50 (2)*	N(1b)	7601 (13)	-1511 (10)	6608 (3)	36 (5)*
S(3)	7589 (5)	2332 (4)	8830 (1)	52 (2)*	N(2b)	7520 (13)	-2611 (11)	6545 (3)	40 (6)*
S(4)	11145 (5)	604 (4)	8685 (1)	54 (2)*	N(3b)	7037 (10)	-854 (8)	5715 (3)	26 (4)*
S(5)	7641 (4)	1037 (3)	9675 (1)	37 (2)*	N(4b)	6937 (15)	-1984 (13)	5787 (3)	49 (7)*
S(6)	9774 (4)	2231 (3)	9648 (1)	37 (2)*	C(1b)	7393 (23)	468 (21)	7540 (6)	85 (6)
S(7)	11976 (4)	-690 (4)	9536 (1)	38 (2)*	C(2b)	8911 (23)	110 (21)	7475 (6)	86 (6)
S(8)	14094 (8)	-4047 (5)	10038 (2)	110 (3)*	C(3b)	7369 (18)	2141 (16)	4920 (5)	53 (4)
N(1)	9978 (12)	-1629 (9)	10039 (4)	37 (5)*	C(4b)	5946 (18)	2122 (16)	4938 (5)	58 (4)
N(2)	9931 (12)	-2739 (11)	9963 (4)	40 (5)*	C(5b)	5523 (18)	3641 (15)	6323 (5)	49 (4)
N(3)	9430 (12)	-957 (9)	9145 (3)	33 (4)*	C(6b)	4346 (18)	3054 (16)	6313 (5)	55 (4)
N(4)	9268 (14)	-2134 (11)	9222 (4)	51 (5)*	C(7b)	10469 (18)	-2498 (16)	6086 (5)	56 (4)
C(1)	9651 (22)	288 (23)	10947 (6)	87 (6)	C(8b)	11769 (22)	-3149 (20)	5822 (6)	79 (6)
C(2)	11148 (17)	179 (15)	10881 (4)	51 (4)	C(11b)	6670 (12)	-2227 (9)	5132 (3)	53 (4)
C(3)	9791 (28)	1725 (26)	8333 (8)	118 (8)	C(12b)	6318 (12)	-2873 (9)	4856 (3)	51 (4)
C(4)	8462 (26)	2176 (25)	8363 (7)	98 (7)	C(13b)	5908 (12)	-3904 (9)	4954 (3)	72 (6)
C(5)	6763 (18)	2889 (16)	9745 (5)	55 (4)	C(14b)	5850 (12)	-4289 (9)	5328 (3)	60 (5)
C(6)	7882 (16)	3452 (14)	9730 (4)	44 (4)	C(15b)	6202 (12)	-3644 (9)	5605 (3)	43 (4)
C(7)	12785 (21)	-2468 (18)	9392 (6)	74 (5)	C(16b)	6611 (12)	-2612 (9)	5507 (3)	38 (4)
C(8)	14193 (23)	-3454 (20)	9564 (6)	86 (6)	C(21b)	7605 (11)	-4755 (9)	6776 (2)	43 (4)
C(11)	10841 (12)	-3718 (9)	10601 (3)	56 (4)	C(22b)	7909 (11)	-5792 (9)	7059 (2)	53 (4)
C(12)	11154 (12)	-4779 (9)	10877 (3)	66 (5)	C(23b)	8462 (11)	-5701 (9)	7402 (2)	57 (4)
C(13)	10876 (12)	-5887 (9)	10810 (3)	69 (5)	C(24b)	8711 (11)	-4573 (9)	7463 (2)	60 (4)
C(14)	10285 (12)	-5932 (9)	10468 (3)	50 (4)	C(25b)	8408 (11)	-3536 (9)	7180 (2)	41 (4)
C(15)	9972 (12)	-4870 (9)	10192 (3)	47 (4)	C(26b)	7855 (11)	-3627 (9)	6837 (2)	27 (3)
C(16)	10250 (12)	-3763 (9)	10259 (3)	29 (3)	N(11)	777 (17)	2314 (15)	5453 (4)	69 (4)
C(21)	8424 (11)	-3711 (9)	9048 (2)	49 (4)	C(31)	394 (31)	4219 (28)	5931 (8)	123 (9)
C(22)	7891 (11)	-4245 (9)	8780 (2)	70 (5)	C(32)	1237 (23)	2943 (20)	5133 (6)	86 (6)
C(23)	7650 (11)	-3672 (9)	8415 (2)	89 (6)	C(33)	-236 (27)	3377 (25)	5739 (7)	101 (7)
C(24)	7943 (11)	-2565 (9)	8317 (2)	75 (5)	C(34)	-101 (25)	3955 (22)	4927 (7)	95 (7)
C(25)	8476 (11)	-2031 (9)	8585 (2)	54 (4)	C(35)	2065 (28)	1204 (26)	5675 (7)	107 (8)
C(26)	8717 (11)	-2604 (9)	8950 (2)	33 (3)	C(36)	2912 (30)	-47 (27)	5429 (8)	121 (9)
Mo(1a)	1799 (1)	11517 (1)	3478 (1)	29 (1)*	N(12)	6267 (17)	2621 (15)	2189 (4)	70 (4)
Mo(2a)	1356 (2)	12080 (1)	2695 (1)	29 (1)*	C(41)	5140 (36)	3232 (33)	2454 (10)	144 (11)
S(1a)	283 (4)	11260 (4)	3999 (1)	41 (2)*	C(42)	4354 (26)	3207 (23)	1632 (7)	94 (7)
S(2a)	3823 (4)	9725 (4)	3861 (1)	43 (2)*	C(43)	5250 (28)	4513 (25)	2655 (7)	104 (8)
S(3a)	-721 (5)	12634 (4)	2252 (1)	50 (2)*	C(44)	6045 (27)	2961 (25)	1798 (7)	102 (8)
S(4a)	2839 (5)	10855 (4)	2159 (1)	49 (2)*	C(45)	7456 (37)	22 (34)	2467 (10)	152 (11)
S(5a)	3729 (4)	11039 (3)	3015 (1)	35 (2)*	C(46)	6462 (27)	1021 (25)	2273 (7)	108 (7)
S(6a)	1590 (4)	9851 (3)	3040 (1)	37 (2)*	N(13)	3012 (20)	2143 (18)	8783 (6)	91 (5)
S(7a)	-640 (4)	12800 (4)	3159 (1)	36 (2)*	C(51)	3710 (50)	2335 (45)	8485 (13)	216 (17)
S(8a)	-2211 (7)	15182 (5)	3940 (1)	90 (3)*	C(52)	2921 (47)	2538 (44)	8088 (12)	206 (16)
N(1a)	1856 (13)	13088 (9)	3560 (3)	42 (4)*	C(53)	5006 (34)	-163 (31)	9053 (9)	139 (10)
N(2a)	2113 (11)	14152 (9)	3492 (3)	35 (4)*	C(54)	4512 (46)	1140 (42)	9032 (12)	197 (16)
N(3a)	1320 (11)	13716 (11)	2664 (3)	33 (5)*	C(55)	2703 (32)	4258 (29)	9166 (9)	132 (10)
N(4a)	1472 (14)	14827 (12)	2727 (3)	42 (6)*	C(56)	2147 (30)	3316 (27)	9013 (8)	118 (8)
C(1a)	1547 (17)	10085 (15)	4357 (4)	46 (4)	N(14)	8255 (15)	9831 (13)	3813 (4)	58 (4)
C(2a)	3084 (18)	10154 (16)	4322 (5)	52 (4)	C(61)	6875 (24)	10990 (22)	3614 (6)	85 (6)
C(3a)	86 (20)	11926 (17)	1809 (5)	64 (5)	C(62)	9066 (27)	8374 (25)	4402 (7)	106 (7)
C(4a)	1614 (17)	11801 (15)	1781 (4)	46 (4)	C(63)	9220 (22)	8898 (19)	3540 (6)	76 (5)
C(5a)	3520 (17)	8567 (15)	2962 (4)	43 (4)	C(64)	8663 (28)	7827 (26)	3415 (7)	111 (8)
C(6a)	4563 (16)	9176 (14)	2957 (4)	45 (4)	C(65)	7716 (29)	9158 (27)	4169 (8)	115 (8)
C(7a)	-1469 (15)	14725 (13)	3205 (4)	33 (3)	C(66)	6108 (27)	12147 (25)	3819 (7)	103 (8)
C(8a)	-2792 (22)	15201 (19)	3465 (6)	76 (5)	N(15)	2808 (16)	9604 (14)	7100 (4)	67 (4)
C(11a)	1373 (11)	16968 (9)	2507 (2)	41 (4)	C(71)	2149 (27)	11628 (25)	7091 (7)	104 (7)
C(12a)	1089 (11)	18000 (9)	2224 (2)	59 (4)	C(72)	3689 (33)	7871 (30)	6579 (9)	129 (10)
C(13a)	561 (11)	17901 (9)	1878 (2)	50 (4)	C(73)	2980 (24)	9187 (21)	7515 (6)	84 (6)
C(14a)	317 (11)	16771 (9)	1815 (2)	71 (5)	C(74)	4444 (39)	8957 (36)	7702 (10)	166 (12)
C(15a)	601 (11)	15740 (9)	2098 (2)	44 (4)	C(75)	1579 (31)	12027 (29)	6772 (8)	129 (9)
C(16a)	1129 (11)	15838 (9)	2444 (2)	32 (3)	C(76)	4032 (32)	8135 (30)	6933 (9)	138 (10)
C(21a)	2775 (12)	15839 (9)	3668 (2)	47 (4)	N(16)	4954 (17)	-111 (15)	549 (4)	76 (4)
C(22a)	3122 (12)	16503 (9)	3940 (2)	68 (5)	C(81)	4542 (25)	1502 (22)	517 (7)	93 (7)
C(23a)	3090 (12)	16120 (9)	4316 (2)	55 (4)	C(82)	6596 (28)	-661 (25)	1130 (7)	107 (7)
C(24a)	2711 (12)	15072 (9)	4420 (2)	52 (4)	C(83)	5308 (23)	-652 (21)	956 (6)	83 (6)
C(25a)	2364 (12)	14408 (9)	4148 (2)	36 (4)	C(84)	6294 (34)	-2204 (31)	243 (9)	139 (10)
C(26a)	2396 (12)	14791 (9)	3772 (2)	33 (3)	C(85)	3801 (27)	2072 (25)	127 (7)	107 (7)
Mo(1b)	7644 (2)	110 (1)	6577 (1)	33 (1)*	C(86)	6141 (38)	-823 (35)	259 (11)	164 (12)
Mo(2b)	7205 (2)	670 (1)	5797 (1)	31 (1)*	N(17)	7004 (26)	6962 (24)	2203 (7)	133 (8)
S(1b)	6151 (4)	1314 (4)	7116 (1)	47 (2)*	N(18)	5641 (23)	7314 (21)	2039 (6)	119 (7)
S(2b)	9708 (4)	-449 (5)	7021 (1)	52 (2)*	C(91)	4368 (12)	7038 (13)	1528 (4)	88 (6)
S(3b)	5193 (4)	2472 (4)	5412 (1)	47 (2)*	C(92)	4287 (12)	6488 (13)	1194 (4)	112 (8)
S(4b)	8707 (4)	927 (4)	5282 (1)	40 (2)*	C(93)	5583 (12)	5563 (13)	1019 (4)	116 (9)
S(5b)	5277 (4)	1157 (4)	6256 (1)	39 (2)*	C(94)	6959 (12)	5188 (13)	1180 (4)	87 (6)

Table III (Continued)

atom	x	y	z	$U_{eq/iso}^a$	atom	x	y	z	$U_{eq/iso}^a$
C(95)	7041 (12)	5738 (13)	1514 (4)	78 (6)	C(02)	2009 (12)	6891 (13)	8093 (4)	91 (6)
C(96)	5745 (12)	6663 (13)	1688 (4)	61 (5)	C(03)	3342 (12)	6383 (13)	8289 (4)	106 (7)
N(19)	2068 (23)	5296 (21)	7042 (6)	117 (7)	C(04)	4649 (12)	5372 (13)	8139 (4)	91 (6)
N(20)	3324 (25)	4890 (22)	7245 (7)	123 (7)	C(05)	4624 (12)	4870 (13)	7793 (4)	103 (7)
C(01)	1984 (12)	6388 (14)	7747 (4)	77 (6)	C(06)	3291 (12)	5378 (13)	7596 (4)	85 (6)

^a An asterisk denotes the equivalent isotropic U for anisotropically refined atoms defined as one-third of the trace of the orthogonalized U_{eq} tensor. Other values are U_{iso} .

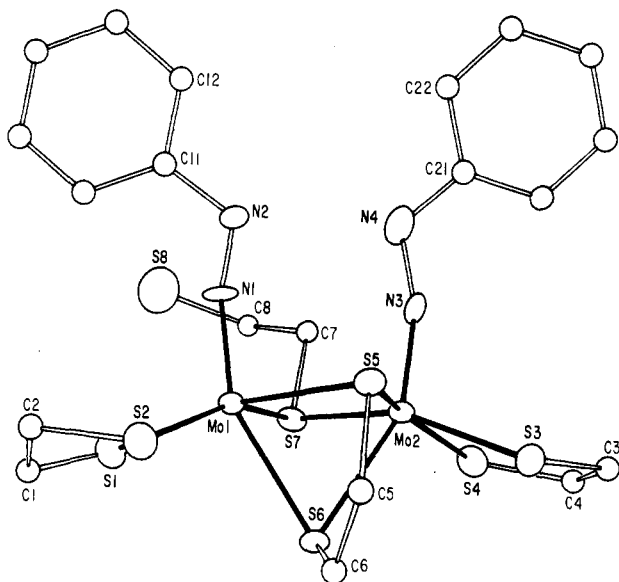
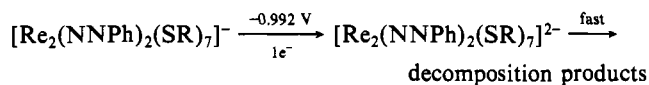


Figure 1. ORTEP view of the structure of $[\text{Mo}_2(\text{NNPh})(\text{NNHPh})(\text{SCH}_2\text{CHS})_3(\text{SCH}_2\text{CH}_2\text{SH})]^{2-}$ (**2**⁻) showing the labeling.

In an attempt to prepare analogous rhenium complexes, $[\text{ReCl}(\text{NNPh})_2(\text{PPh}_3)_2]^{22}$ was reacted with a variety of monodentate, bidentate, and sterically hindered thiolate ligands. Only from the reaction with thiophenol was a tractable material isolable, yielding the anionic rhenium(II) complex $[\text{Re}_2(\text{NNPh})_2(\text{SPh})_7]^-$, isolated as the triethylammonium salt (**4**). The red diamagnetic complex exhibits ¹H NMR integration consistent with the empirical formulation, and a conductivity measurement showed ionization of a 1:1 electrolyte in acetonitrile solution.

The band at 1640 cm^{-1} in the infrared spectrum of **4** is assigned to $\nu(\text{NN})$. The electronic spectrum exhibits a band at 410 nm associated with the $[\text{Re}(\text{NNR})]$ chromophore.

The electrochemistry of complexes **1–4** has been briefly studied by cyclic voltammetry and controlled potential electrolysis. The results are presented in Table II. Complexes **2** and **4** exhibit similar electrochemical characteristics, presenting an irreversible one-electron reduction at about -1.00 V and an irreversible one-electron oxidation at ca. $+0.90\text{ V}$. The behavior of $[\text{Re}_2(\text{NNPh})_2(\text{SR})_7]^-$ (**4**⁻) in the cathodic range is similar to that observed for $[\text{Re}_2(\text{NO})_2(\text{SR})_7]^-$,¹² which exhibits an irreversible one-electron reduction at -1.25 V . The behavior is consistent with the rapid decomposition of the reduced species $[\text{Re}_2(\text{NNPh})_2(\text{SR})_7]^{2-}$ to electrochemically inactive products:



This observation is consistent with the structural analysis and the molecular orbital description of **4**, which indicates that upon reduction the electron would populate the LUMO, an orbital strongly antibonding with respect to the bridge interaction (see below and Figure 4). The irreversible nature of the anodic process at $+0.849\text{ V}$ may also be explained in terms of Figure 4. Removal of an electron from the HOMO, the metal-metal-bonding a_1 orbital, would weaken an effectively bridge-stabilizing interaction and may account for the instability of the neutral anodic product

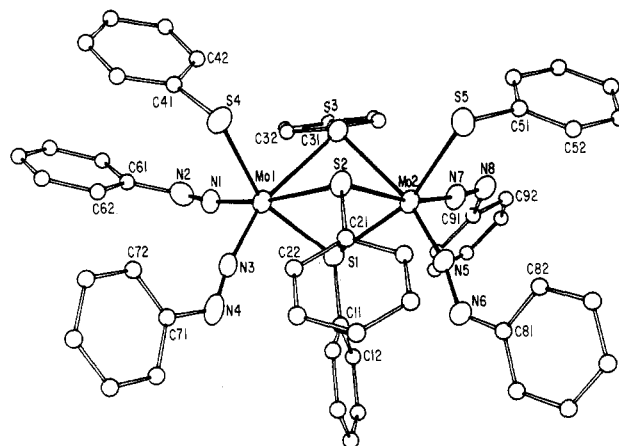


Figure 2. Perspective view of the structure of $[\text{Mo}_2(\text{NNPh})_4(\text{SPh})_5]^{3-}$ (**3a**⁻) with atom labeling.

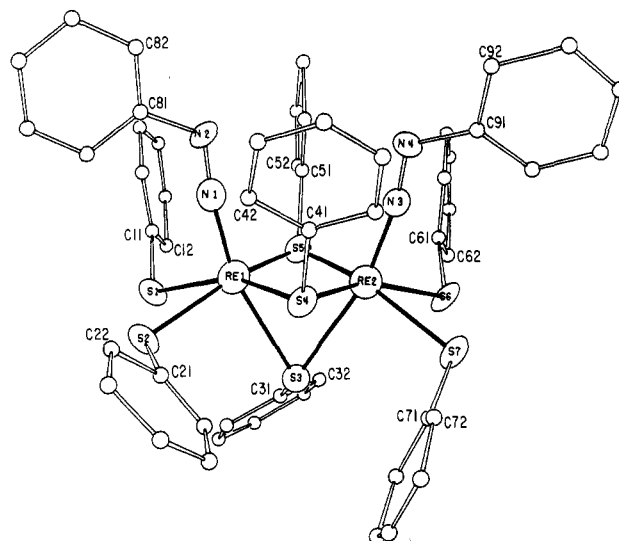


Figure 3. ORTEP diagram of the structure of $[\text{Re}_2(\text{NNPh})_2(\text{SPh})_7]^-$ (**4**⁻).

$[\text{Re}_2(\text{NNPh})_2(\text{SR})_7]$ on the cyclic voltammetric time scale. The Mo complex **2** exhibits structural characteristics similar to those of **4** and may be described in terms of the same bonding picture (vide infra). The data of Table II confirm that the electrochemical characteristics of **2** and **4** are similar.

In contrast, complex **3a** exhibits a complex pattern of quasi-reversible and irreversible anodic processes in the cyclic voltammetry. The quasi-reversible nature of the oxidations at $+0.552$ and $+0.696\text{ V}$ suggests that the HOMO is not intimately involved in the bridge bonding, an observation consistent with the absence of a metal-metal bond in the structure of **3a** and with the molecular orbital description presented in Figure 4. The subsequent multielectron oxidation results in decomposition of the product:

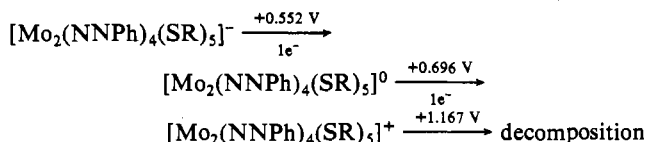


Table IV. Atom Coordinates ($\times 10^4$) and Temperature Factors ($\text{\AA}^2 \times 10^3$) for $[\text{HNEt}_3][\text{Mo}_2(\text{NNPh})_4(\text{SPh})_3]$ (**3a**)

atom	x	y	z	$U_{\text{eq/iso}}^a$	atom	x	y	z	$U_{\text{eq/iso}}^a$
Mo(1)	1986 (1)	6120 (1)	8249 (1)	43 (1)*	C(35)	2594 (18)	9026 (15)	9896 (8)	141 (6)
Mo(2)	992 (1)	6801 (1)	6939 (1)	41 (1)*	C(36)	1945 (14)	8197 (12)	9437 (6)	102 (5)
S(1)	1610 (2)	7990 (2)	7872 (1)	45 (1)*	C(41)	-1107 (12)	8132 (11)	6385 (5)	75 (3)
S(2)	-179 (3)	5424 (2)	7700 (1)	48 (1)*	C(42)	-1724 (15)	7776 (14)	5880 (7)	116 (5)
S(3)	3028 (2)	6540 (2)	7311 (1)	46 (1)*	C(43)	-1628 (21)	8651 (18)	5480 (9)	173 (8)
S(4)	490 (3)	6044 (3)	9006 (1)	61 (1)*	C(44)	-1000 (15)	9723 (13)	5642 (7)	125 (6)
S(5)	-1171 (3)	7037 (3)	6878 (1)	59 (1)*	C(45)	-480 (15)	10177 (14)	6097 (7)	116 (5)
N(1)	2214 (8)	4695 (7)	8288 (3)	49 (4)*	C(46)	-529 (16)	9266 (14)	6496 (7)	120 (5)
N(2)	2460 (9)	3793 (8)	8236 (4)	67 (4)*	C(51)	1920 (10)	2857 (8)	8607 (4)	54 (3)
N(3)	3429 (8)	6752 (7)	8690 (3)	45 (3)*	C(52)	1371 (10)	2976 (9)	9091 (4)	61 (3)
N(4)	4409 (8)	7156 (7)	8980 (3)	60 (4)*	C(53)	875 (12)	2017 (11)	9409 (5)	82 (4)
N(5)	1735 (7)	7989 (6)	6481 (3)	43 (3)*	C(54)	969 (13)	980 (12)	9250 (6)	96 (4)
N(6)	2070 (8)	8821 (7)	6170 (3)	49 (4)*	C(55)	1506 (13)	841 (12)	8772 (5)	91 (4)
N(7)	751 (7)	5679 (7)	6389 (3)	48 (3)*	C(56)	2014 (11)	1797 (9)	8434 (5)	69 (3)
N(8)	800 (9)	4900 (7)	6080 (3)	58 (4)*	C(61)	4446 (11)	6902 (9)	9537 (4)	61 (3)
N(9)	2588 (9)	2976 (8)	1957 (4)	77 (5)*	C(62)	5322 (13)	7673 (12)	9901 (6)	93 (4)
C(1)	3037 (10)	9241 (8)	7825 (4)	51 (3)	C(63)	5402 (15)	7445 (13)	10462 (7)	117 (5)
C(2)	4002 (13)	9465 (11)	8211 (5)	91 (4)	C(64)	4778 (18)	6396 (15)	10619 (8)	139 (6)
C(3)	5097 (16)	10548 (14)	8195 (7)	123 (5)	C(65)	3874 (19)	5563 (16)	10305 (8)	147 (7)
C(4)	5134 (14)	11242 (12)	7754 (6)	95 (4)	C(66)	3728 (14)	5848 (12)	9730 (6)	100 (5)
C(5)	4198 (13)	11082 (11)	7390 (5)	85 (4)	C(71)	3421 (9)	9349 (8)	6048 (4)	47 (3)
C(6)	3123 (11)	10039 (9)	7433 (5)	66 (3)	C(72)	3695 (11)	10353 (9)	5733 (4)	62 (3)
C(11)	-787 (10)	3947 (8)	7489 (4)	54 (3)	C(73)	4995 (12)	10910 (10)	5605 (5)	75 (4)
C(12)	-700 (12)	3090 (10)	7833 (5)	76 (4)	C(74)	5924 (12)	10471 (10)	5757 (5)	73 (3)
C(13)	-1203 (15)	1899 (13)	7649 (7)	111 (5)	C(75)	5634 (12)	9498 (10)	6063 (5)	77 (4)
C(14)	-1802 (15)	1647 (14)	7148 (7)	110 (5)	C(76)	4360 (10)	8934 (9)	6212 (4)	60 (3)
C(15)	-2024 (15)	2442 (13)	6821 (6)	107 (5)	C(81)	-274 (10)	4350 (8)	5701 (4)	49 (3)
C(16)	-1474 (12)	3623 (10)	6994 (5)	76 (4)	C(82)	-1281 (10)	4701 (9)	5648 (4)	63 (3)
C(21)	3307 (10)	5357 (9)	6958 (4)	57 (3)	C(83)	-2301 (13)	4118 (10)	5256 (5)	85 (4)
C(22)	2527 (11)	4223 (9)	6962 (5)	68 (3)	C(84)	-2133 (13)	3212 (11)	4949 (5)	82 (4)
C(23)	2791 (14)	3328 (12)	6678 (5)	95 (4)	C(85)	-1149 (12)	2867 (10)	5001 (5)	77 (4)
C(24)	3894 (16)	3645 (14)	6388 (6)	117 (5)	C(86)	-160 (11)	3422 (9)	5375 (5)	68 (3)
C(25)	4737 (18)	4749 (15)	6374 (7)	132 (6)	Cn(1)	3654 (14)	2571 (12)	2099 (6)	116 (5)
C(26)	4417 (14)	5649 (12)	6655 (5)	96 (4)	Cn(2)	3321 (15)	1471 (12)	2417 (6)	112 (5)
C(31)	1304 (12)	7033 (10)	9549 (5)	73 (3)	Cn(3)	3119 (16)	4176 (13)	1703 (7)	135 (6)
C(32)	1348 (14)	6629 (13)	10097 (6)	101 (5)	Cn(4)	3791 (14)	5096 (11)	2116 (6)	107 (5)
C(33)	2008 (17)	7447 (16)	10524 (8)	137 (6)	Cn(5)	1557 (16)	2206 (13)	1588 (6)	125 (6)
C(34)	2579 (18)	8571 (16)	10407 (8)	137 (6)	Cn(6)	1957 (19)	1935 (16)	1032 (7)	168 (8)

^aAn asterisk denotes the equivalent isotropic U for anisotropically refined atoms defined as one-third of the trace of the orthogonalized u_{eq} tensor. Other values are U_{iso} .

Reduction of **3a** occurs at highly negative potentials in comparison to the anodic processes for **2** and **4**. Since the LUMO is presumably strongly antibonding in character, the irreversibility and relative difficulty of reduction appear to be consistent with the general bonding description of this species.

Description of the Structures. The structures of three examples of triply bridged binuclear metal diazenido complexes have been determined. Tables III–V give atomic coordinates for the structures of **2**, **3a**, and **4**, respectively, and the structures are illustrated in Figures 1–3. Selected bond lengths and angles are presented in Tables VI–VIII.

The structure of **2** consists of discrete binuclear complex anions with pseudooctahedral molybdenum atoms sharing a face defined by three bridging thiolate sulfur donors. The coordination about each molybdenum atom is completed by this thiolate sulfur atoms of the terminal chelating dimercaptoethane ligands and by the σ -nitrogen donors of the terminally coordinated organodiazenido and organohydrazido moieties.

The structure presents three structurally distinct types of dimercaptoethane ligands: two terminally coordinating chelating groups, a doubly bridging ligand, and a dimercaptoethane group bridging through a single thiolate donor, leaving an uncoordinated thiol function. A similar coordination pattern has been observed in the structure of $[\text{Pr}_3\text{NH}][\text{Mo}_2\text{O}_2(\text{SCH}_2\text{CH}_2\text{O})_3(\text{SCH}_2\text{CH}_2\text{O}-\text{H})]$; although in this latter instance, the nonbridging 2-hydroxyethanethiolate ligand occupies a nonbridging position in the molybdenum coordination sphere.

An unusual feature of the structure is the occupancy of the Z position, the bridge position trans to the strongly π -bonded hydrazido ligands, by a thiolate donor. Although examples of the Z position occupied by Cl^- , OR^- , NR_2^- , or SR^- have been described, RS^- groups do not favor the Z position, most likely as

a consequence of competition for the metal π -orbital by the strongly π -donating thiolate ligand and the π -bonding trans oxo-organodiazenido groups.²⁶ Thus, $[\text{Mo}_2\text{O}_3(\text{SPh})_2(\text{S}_2\text{CNET}_2)_2]$ is very reactive⁵ and $[\text{Mo}_2\text{O}_2(\text{SAr})_7]^-$ could not be isolated.⁷ The stability of **2**, a species with a triply bridging thiolate geometry, may suggest that π -donation to the diazenido ligand, $-\text{NNR}$, is particularly strong and effectively favors trans-thiolate coordination, in contrast to the strongly π -donating oxo group. The trans influence of the organodiazenido and organohydrazido ligands is suggested by the significantly elongated Mo–S(6) distances, 2.577 (8) Å (av), compared to an average value of 2.457 (8) Å for all other Mo–S distances in the binuclear unit. Although not as pronounced as that associated with oxo groups, the trans influence of the arylidiazene group has also been documented in complexes of the type $[\text{Mo}(\text{N}_2\text{Ar})(\text{S}_2\text{CNR}_2)_3]$.³⁴ Such lengthening of an axial metal ligand bond trans to a multiply bonded group, relative to equatorial metal–ligand bond distances, is generally observed.³⁵

A further consequence of the competition for the metal t_{2g} -type orbitals by the mercapto sulfur and the hydrazido nitrogen is shown by the orientation of the $-\text{NNHR}$ and $-\text{NNR}$ groupings, whose planes are rotated ca. 27° from the eclipsing conformation relative to the S(1)–Mo(1)–S(5) and the S(4)–Mo(2)–S(7) vector projections. This orientation is intermediate between the fully eclipsed orientation of mononuclear NNR_2 or NNR complexes where metal–hydrazido bonding is maximized²⁷ and the 40° orientation that bisects the bond angles in the tetragonal plane found for $[\text{Mo}_3\text{S}_8(\text{NNMe}_2)_2]^{2-}$,²⁸ where there is no net overlap

(34) Butler, G.; Chatt, J.; Leigh, G. J.; Smith, A. R. P.; Williams, G. A. *Inorg. Chim. Acta* **1978**, *28*, L165.

(35) Drew, M. G. B. *Prog. Inorg. Chem.* **1977**, *23*, 67.

Table V. Atom Coordinates ($\times 10^4$) and Temperature Factors ($\text{\AA}^2 \times 10^3$) for 4

atom	x	y	z	U_{iso}^a	atom	x	y	z	U_{iso}^a
Re(1)	10353 (1)	-567 (1)	2490 (1)	38 (1)*	C(51)	12776 (21)	150 (9)	3375 (11)	38 (7)
Re(2)	10016 (1)	513 (1)	2439 (1)	40 (1)*	C(52)	13526 (22)	179 (10)	2971 (12)	54 (8)
S(1)	9439 (6)	-90 (3)	1672 (3)	40 (3)*	C(53)	14802 (23)	231 (10)	3191 (12)	49 (8)
S(2)	9183 (7)	-1346 (3)	2100 (4)	59 (3)*	C(54)	15238 (29)	269 (12)	3759 (14)	76 (10)
S(7)	8388 (7)	1105 (3)	1950 (4)	60 (3)*	C(55)	14489 (27)	219 (11)	4144 (14)	72 (10)
S(3)	8441 (6)	-116 (3)	2729 (3)	46 (3)*	C(56)	13219 (25)	166 (11)	3952 (12)	62 (9)
S(5)	11146 (6)	45 (3)	3234 (3)	42 (3)*	C(61)	11287 (28)	1334 (13)	3589 (15)	78 (10)
S(6)	9870 (7)	1263 (3)	3075 (4)	68 (4)*	C(62)	12379 (31)	1399 (13)	3383 (16)	97 (12)
S(1)	10538 (7)	-1241 (4)	3235 (4)	63 (4)*	C(63)	13485 (44)	1522 (18)	3727 (22)	161 (19)
N(3)	11306 (17)	785 (8)	2155 (10)	41 (8)*	C(64)	13325 (36)	1615 (16)	4283 (18)	115 (14)
N(4)	12235 (18)	891 (9)	1956 (10)	53 (10)*	C(65)	12337 (37)	1612 (17)	4527 (19)	135 (16)
N(1)	11818 (21)	-702 (8)	2273 (8)	48 (9)*	C(66)	11147 (39)	1488 (17)	4090 (19)	138 (16)
N(2)	12821 (20)	-724 (8)	2100 (10)	53 (11)*	C(11)	11977 (22)	-1204 (11)	3683 (12)	51 (8)
C(41)	10419 (21)	-37 (13)	1145 (10)	45 (7)	C(12)	13103 (26)	-1246 (13)	3560 (15)	84 (11)
C(42)	10495 (21)	441 (12)	881 (11)	53 (8)	C(13)	14253 (34)	-1228 (15)	3918 (17)	103 (13)
C(43)	11135 (23)	475 (13)	433 (12)	66 (9)	C(14)	14223 (39)	-1070 (16)	4428 (19)	127 (16)
C(44)	11665 (23)	62 (13)	261 (11)	61 (8)	C(15)	13198 (6)	-1050 (16)	4652 (19)	134 (16)
C(45)	11618 (24)	-399 (13)	531 (13)	67 (9)	C(16)	11953 (32)	-1081 (14)	4272 (15)	103 (13)
C(46)	10964 (22)	-478 (13)	975 (12)	64 (9)	C(91)	12225 (24)	1409 (11)	1682 (12)	56 (8)
C(21)	8276 (24)	-1239 (12)	1434 (12)	59 (8)	C(92)	11522 (24)	1840 (12)	1825 (13)	66 (9)
C(22)	8626 (28)	-1581 (13)	989 (14)	81 (10)	C(93)	11542 (33)	2323 (16)	1523 (16)	108 (13)
C(23)	7852 (27)	-1611 (13)	455 (14)	78 (10)	C(94)	12425 (33)	2437 (17)	1206 (16)	111 (13)
C(24)	6882 (28)	-1278 (13)	363 (15)	83 (11)	C(95)	13177 (33)	2052 (16)	1101 (16)	111 (13)
C(25)	6561 (27)	-942 (13)	756 (13)	75 (10)	C(96)	13112 (28)	1497 (14)	1349 (14)	84 (11)
C(26)	7292 (23)	-945 (11)	1292 (12)	54 (8)	C(81)	13192 (24)	-1213 (11)	1896 (12)	49 (8)
C(71)	7125 (25)	791 (12)	1527 (13)	65 (9)	C(82)	12549 (26)	-1666 (13)	1963 (13)	66 (9)
C(72)	6213 (25)	524 (13)	1768 (14)	84 (10)	C(83)	12968 (35)	-2100 (17)	1757 (17)	119 (15)
C(73)	5144 (32)	301 (14)	1395 (17)	99 (12)	C(84)	13990 (39)	-2107 (18)	1520 (18)	132 (16)
C(74)	5120 (34)	327 (15)	862 (18)	107 (13)	C(85)	14682 (40)	-1677 (19)	1556 (18)	137 (16)
C(75)	5906 (33)	555 (16)	575 (17)	117 (13)	C(86)	14203 (30)	-1204 (15)	1699 (14)	91 (12)
C(76)	6973 (34)	738 (15)	911 (17)	113 (14)	N	7177 (25)	2117 (15)	2569 (14)	155 (20)*
C(31)	8359 (23)	-214 (11)	3458 (12)	51 (8)	C(1)	5951 (43)	1870 (20)	2566 (23)	202 (24)
C(32)	8725 (24)	178 (12)	3853 (13)	65 (9)	C(2)	4890 (34)	2301 (17)	2536 (18)	160 (19)
C(33)	8663 (24)	79 (13)	4444 (12)	67 (9)	C(3)	7504 (41)	2339 (17)	3123 (19)	168 (20)
C(34)	8172 (27)	-403 (14)	4553 (16)	90 (11)	C(4)	7419 (41)	1953 (18)	3583 (21)	186 (22)
C(35)	7792 (30)	-763 (16)	4154 (16)	106 (13)	C(5)	7012 (48)	2522 (21)	2033 (22)	211 (25)
C(36)	7902 (26)	-698 (13)	3571 (14)	82 (11)	C(6)	8398 (50)	2738 (22)	2247 (25)	265 (33)

^a An asterisk denotes the equivalent isotropic U defined as one-third of the trace of the orthogonalized U_{eq} tensor.

of the Mo t_{2g} -type orbitals with the nitrogen p orbitals. The metal-hydrazido grouping is apparently stabilized by hydrogen bonding between the β -nitrogen N(2) and the terminal nitrogen N(4) of the phenyldiazenido group. As a consequence, the $[\text{Mo}_2(\text{NNHPh})(\text{NNPh})]$ grouping is planar, with the seven-membered ring Mo(1)-N(1)-N(2)-H...N(4)-N(3)-Mo(2) displaying considerable distortion from linearity of the Mo-N-N moieties, such that the -NPh and -NHPh units bend toward each other.

The hydrazido(2-) fragment, -NNHPh, functions formally as a four-electron donor, consistent with canonical forms I and II. This description is consistent with short Mo(1)-N(1) and N(1)-N(2) distances and the "linearity" of the Mo(1)-N(1)-N(2) unit. The other nitrogenous fragment, -NNR, functions as a three-electron donor and may be described as the organodiazenido ligand, (NNR)⁺, a species isoelectronic with NO.²⁹ With this formalism, the Mo oxidation states are +3. Alternatively, the -NNR grouping may be described as the hydrazido(3-) ligand, and the molybdenum oxidation states as +5. This latter description possesses the advantage of yielding a formal metal oxidation state consistent with that for other examples of triply bridged binuclear molybdenum complexes but provides a rather inadequate description of the -NNR linkage. The ambiguity is a consequence of the "noninnocent" nature of the organodiazenido ligand and the inadequacy of valence formalism in describing its structure.

The asymmetry of the triple thiolato bridge implies the existence of a metal-metal bond, consistent with the short Mo-Mo distance of 2.839 (2) Å and with the observed diamagnetism of the complex. Each molybdenum attains a formal 18-electron configuration by formation of a Mo-Mo bond. Thus, if the hydrazido(2-) and the diazenido ligands contribute four and three electrons, respectively, each terminal thiolate one, each bridging thiolate three, and each molybdenum six, the overall dinegative charge brings

the total electron count to 34. If a σ bond is allocated to each terminal ligand, two σ bonds to each bridging thiolate, and two π bonds to each Mo-N group, there are 16 metal-ligand bonding orbitals occupied by 32 electrons and a Mo-Mo bonding orbital occupied by two electrons, as illustrated schematically in Figure 4.

The six thiolate sulfurs cis to the NNR and NNHR ligands are bent away from these groups so that the N-Mo-S angles are greater than 90°, resulting in a distortion of the bridge structures to C_{2v} symmetry. The influence of metal-metal bonding on this bridge structure is also apparent. If the structure is viewed in overall geometry as two Mo octahedra sharing a face, geometric distortions may be described in terms of the quantified treatment of facial octahedra by Cotton and Ucko.³⁰ Since 2 lacks the D_{3h} symmetry of the examples discussed by Cotton and Ucko, only the $\beta = 70.53^\circ$ parameter is meaningful. In the absence of a metal-metal bond, this angle deviates from the ideal value of 0° so as to increase the metal-metal distance, as a consequence of the repulsion between the metal centers. Values close to 0° are suggestive of significant metal-metal interactions. The values for 2 of +1.7, +1.9, and -4.5° for S(5), S(7), and S(6), respectively, are consistent with the presence of a metal-metal bond. The significantly more acute angle at S(6) is a consequence of the long Mo-S(6) distances, produced by the trans influence of the strongly π -bonding organohydrazido and organodiazenido ligands.

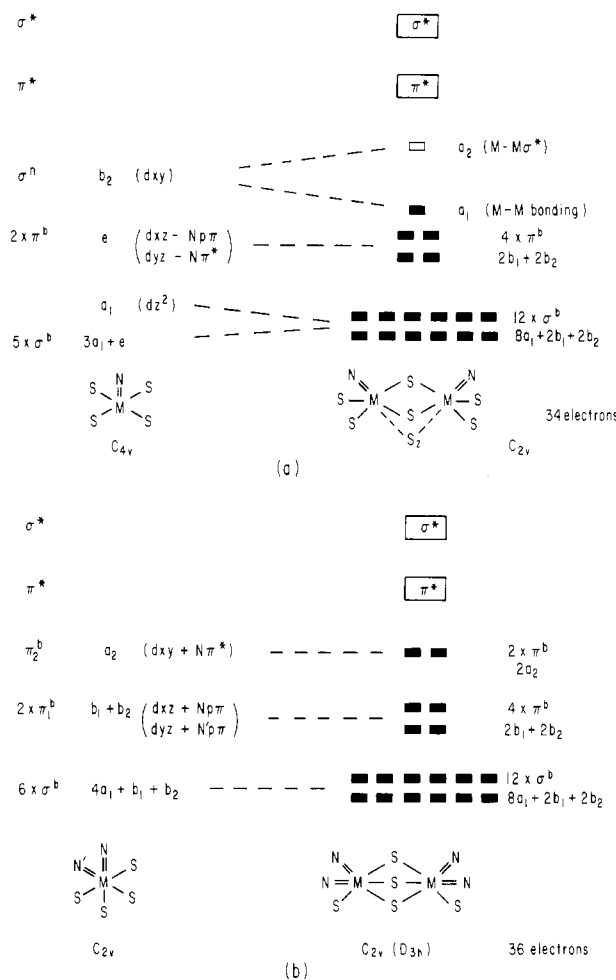
The bridge parameters for 2 are similar to those observed for other examples of triply bridged binuclear complexes of Mo and W, shown in Table VIII, with the exception of $[\text{Mo}_2(\text{NNPh})_4(\text{SPh})_2]^-$ (3a⁻) whose structure will be discussed below. The distortions of these structures from D_{3h} to C_{2v} symmetry suggest a more useful description of the structures as two edge-sharing square pyramids, with an additional weak interaction along the vector trans to the metal- π -ligand axis (Z). The displacement

Table VI. Selected Bond Lengths (Å) and Angles (deg) for [HNEt₃][Mo₂(NNPh)(NNHPh)(SCH₂CH₂S)₃(SCH₂CH₂SH)]·²/₃H₂NNHPh (2)

	anion 1	anion 2	anion 3
Mo(1)–Mo(2)	2.839 (2)	2.842 (2)	2.835 (2)
Mo(1)–S(1)	2.479 (4)	2.492 (5)	2.467 (4)
Mo(1)–S(2)	2.477 (5)	2.449 (3)	2.491 (5)
Mo(1)–S(5)	2.448 (4)	2.432 (4)	2.450 (4)
Mo(1)–S(6)	2.579 (4)	2.552 (4)	2.569 (4)
Mo(1)–S(7)	2.465 (4)	2.483 (4)	2.425 (4)
Mo(1)–N(1)	1.782 (12)	1.775 (12)	1.779 (13)
Mo(2)–S(3)	2.441 (4)	2.495 (2)	2.446 (5)
Mo(2)–S(4)	2.493 (5)	2.472 (4)	2.466 (4)
Mo(2)–S(5)	2.440 (4)	2.418 (4)	2.427 (4)
Mo(2)–S(6)	2.568 (4)	2.566 (4)	2.561 (4)
Mo(2)–S(7)	2.425 (4)	2.466 (4)	2.464 (4)
Mo(2)–N(3)	1.715 (13)	1.751 (14)	1.786 (11)
N(1)–N(2)	1.272 (17)	1.310 (17)	1.271 (20)
N(3)–N(4)	1.382 (19)	1.319 (20)	1.286 (19)
S(1)–Mo(1)–S(2)	81.5 (1)	81.7 (1)	81.7 (1)
S(1)–Mo(1)–S(5)	158.7 (2)	163.1 (1)	164.5 (1)
S(1)–Mo(1)–S(6)	95.1 (2)	98.2 (2)	94.7 (1)
S(1)–Mo(1)–S(7)	83.1 (1)	83.1 (1)	83.9 (1)
S(1)–Mo(1)–N(1)	102.8 (4)	104.4 (4)	103.5 (4)
S(2)–Mo(1)–S(5)	83.9 (1)	84.1 (1)	83.0 (1)
S(2)–Mo(1)–S(6)	98.8 (2)	96.4 (1)	101.3 (2)
S(2)–Mo(1)–S(7)	162.3 (1)	159.8 (2)	164.5 (1)
S(2)–Mo(1)–N(1)	102.0 (4)	103.4 (4)	99.8 (4)
S(5)–Mo(1)–S(6)	71.9 (1)	74.3 (1)	72.6 (1)
S(5)–Mo(1)–S(7)	108.4 (1)	108.3 (1)	109.1 (1)
S(5)–Mo(1)–N(1)	95.4 (4)	87.8 (4)	94.9 (4)
S(6)–Mo(1)–S(7)	74.1 (1)	72.7 (1)	74.3 (1)
S(6)–Mo(1)–N(1)	154.3 (4)	151.7 (4)	153.9 (4)
S(7)–Mo(1)–N(1)	89.8 (4)	93.2 (4)	89.1 (4)
Mo(1)–N(1)–N(2)	164.3 (10)	159.2 (11)	167.0 (10)
Mo(1)–S(5)–Mo(2)	71.0 (1)	71.7 (1)	70.5 (1)
Mo(1)–S(6)–Mo(2)	66.9 (1)	67.5 (1)	67.1 (1)
Mo(1)–S(7)–Mo(2)	71.7 (1)	70.1 (1)	71.5 (1)
S(3)–Mo(2)–S(4)	82.6 (1)	81.5 (1)	81.8 (1)
S(3)–Mo(2)–S(5)	157.8 (2)	164.6 (1)	159.2 (2)
S(3)–Mo(2)–S(6)	95.0 (1)	101.3 (2)	95.9 (1)
S(3)–Mo(2)–S(7)	84.1 (1)	82.7 (1)	83.9 (1)
S(3)–Mo(2)–N(3)	103.9 (3)	98.2 (4)	102.6 (3)
S(4)–Mo(2)–S(5)	82.3 (1)	84.1 (1)	82.8 (1)
S(4)–Mo(2)–S(6)	101.0 (2)	94.3 (1)	97.7 (2)
S(4)–Mo(2)–S(7)	165.5 (1)	157.1 (2)	162.8 (1)
S(4)–Mo(2)–N(3)	102.2 (4)	104.2 (4)	106.3 (4)
S(5)–Mo(2)–S(6)	72.2 (1)	74.3 (1)	72.5 (1)
S(5)–Mo(2)–S(7)	108.6 (1)	109.3 (1)	108.5 (1)
S(5)–Mo(2)–N(3)	95.1 (3)	90.6 (4)	95.0 (3)
S(6)–Mo(2)–S(7)	74.3 (1)	72.8 (1)	74.4 (1)
S(6)–Mo(2)–N(3)	151.6 (3)	154.9 (4)	151.4 (4)
S(7)–Mo(2)–N(3)	86.6 (4)	94.3 (4)	86.0 (4)
Mo(2)–N(3)–N(4)	159.4 (8)	159.2 (11)	159.3 (10)

of the metal atoms of these structures from the well-developed equatorial plane in the direction of the π -ligand is consistent with this description.

The structure of **4** conforms to the geometric principles common to structures of this type. Thus, the overall structure consists of two octahedra sharing a face defined by three bridging thiolate donors. The Re(1)–S(4)–S(5)–Re(2) rhombus is planar, with a short Re(1)–Re(2) distance of 2.747 (2) Å, consistent with significant metal–metal bonding. The Re atoms are displaced from the S_4 equatorial planes in the direction of the diazenido ligands. The thiolate ligand in the Z site displays a significantly longer Re–S distance of 2.536 (7) Å, compared to the average of 2.392 (9) Å, for Re–S distances in the Re₂S₂ rhombus. If we consider the diazenido ligand to function as a three-electron donor, an 18-electron count is attained by the formation of a Re–Re bond. The structural parameters for the Re–NNPh groupings are consistent with this description. The short Re–Re distance and the observed diamagnetism confirm the presence of a strong Re–Re interaction. The gross structural parameters for **4** are essentially identical to those reported for [Re₂(NO)₂(SAr)₇][–], reinforcing the chemical and structural relationship between the

**Figure 4.** Comparison of qualitative molecular orbital schemes (a) for 34-electron structures of the type [M₂L₂(μ-X)(μ-Y)(μ-Z)L'₄]^{m-} and (b) for 36-electron structures of the type [M₂L₄(μ-X)(μ-X)(μ-Y)(μ-Z)L'₂], where L is a strongly π -bonding ligand.**Table VII.** Selected Bond Lengths (Å) and Angles (deg) for [HNEt₃][Mo₂(NNPh)₄(SPh)₅] (3a)

Mo(1)–S(1)	2.622 (3)	Mo(2)–S(1)	2.606 (2)
Mo(1)–S(2)	2.564 (3)	Mo(2)–S(2)	2.573 (3)
Mo(1)–S(3)	2.548 (3)	Mo(2)–S(3)	2.512 (3)
Mo(1)–S(4)	2.475 (3)	Mo(2)–S(5)	2.491 (3)
Mo(1)–N(1)	1.838 (10)	Mo(2)–N(5)	1.813 (7)
Mo(1)–N(3)	1.819 (8)	Mo(2)–N(7)	1.837 (8)
N(1)–N(2)	1.221 (15)	N(5)–N(6)	1.230 (10)
N(3)–N(4)	1.219 (11)	N(7)–N(8)	1.213 (12)
S(1)–Mo(1)–S(2)	73.1 (1)	S(1)–Mo(2)–S(2)	73.3 (1)
S(1)–Mo(1)–S(3)	72.2 (1)	S(1)–Mo(2)–S(3)	73.0 (1)
S(1)–Mo(1)–S(4)	90.3 (1)	S(1)–Mo(2)–S(5)	92.7 (1)
S(1)–Mo(1)–N(1)	162.7 (2)	S(1)–Mo(2)–N(5)	97.8 (2)
S(1)–Mo(1)–N(3)	101.8 (3)	S(1)–Mo(2)–N(7)	163.3 (3)
S(2)–Mo(1)–S(3)	85.9 (1)	S(2)–Mo(2)–S(3)	86.4 (1)
S(2)–Mo(1)–S(4)	80.0 (1)	S(2)–Mo(2)–S(5)	79.4 (1)
S(2)–Mo(1)–N(1)	97.4 (2)	S(2)–Mo(2)–N(5)	168.6 (3)
S(2)–Mo(1)–N(3)	171.9 (3)	S(2)–Mo(2)–N(7)	97.1 (2)
S(3)–Mo(1)–S(4)	160.2 (1)	S(3)–Mo(2)–S(5)	162.3 (1)
S(3)–Mo(1)–N(1)	93.0 (2)	S(3)–Mo(2)–N(5)	97.8 (3)
S(3)–Mo(1)–N(3)	98.7 (2)	S(3)–Mo(2)–N(7)	93.1 (3)
S(4)–Mo(1)–N(1)	102.5 (3)	S(5)–Mo(2)–N(5)	94.3 (3)
S(4)–Mo(1)–N(3)	93.9 (3)	S(5)–Mo(2)–N(7)	99.0 (3)
N(1)–Mo(1)–N(3)	89.1 (4)	N(5)–Mo(2)–N(7)	93.2 (3)
Mo(1)–S(1)–Mo(2)	84.9 (1)		
Mo(1)–S(2)–Mo(2)	86.7 (1)		
Mo(1)–S(3)–Mo(2)	88.4 (1)		
Mo(1)–N(1)–N(2)	169.8 (7)	Mo(2)–N(5)–N(6)	170.7 (8)
Mo(1)–N(3)–N(4)	178.4 (8)	Mo(2)–N(7)–N(8)	166.9 (8)

diazenido grouping and the isoelectronic nitrosyl group as three-electron donor ligands with a strong preference for linear

Table VIII. Selected Bond Lengths (Å) and Angles (deg) for $[\text{HNEt}_3][\text{Re}_2(\text{NNPh})_2(\text{SPh})_7] (4)$

Re(1)-Re(2)	2.747 (2)	Re(2)-S(5)	2.398 (7)
Re(1)-S(1)	2.451 (9)	Re(2)-S(6)	2.459 (8)
Re(1)-S(2)	2.438 (8)	Re(2)-S(7)	2.457 (9)
Re(1)-S(3)	2.539 (7)	Re(1)-N(1)	1.81 (2)
Re(1)-S(4)	2.374 (7)	Re(2)-N(3)	1.81 (2)
Re(1)-S(5)	2.404 (7)	N(1)-N(2)	1.23 (3)
Re(2)-S(3)	2.553 (7)	N(3)-N(4)	1.24 (3)
Re(2)-S(4)	2.390 (7)		
S(1)-Re(1)-S(2)	72.2 (3)	S(6)-Re(2)-S(7)	73.2 (3)
S(1)-Re(1)-S(3)	96.6 (3)	S(6)-Re(2)-S(3)	100.6 (3)
S(1)-Re(1)-S(4)	157.8 (2)	S(6)-Re(2)-S(4)	159.1 (2)
S(1)-Re(1)-S(5)	85.8 (3)	S(6)-Re(2)-S(5)	87.8 (3)
S(1)-Re(1)-N(1)	96.9 (7)	S(1)-Re(1)-N(3)	95.1 (7)
S(2)-Re(1)-S(3)	92.9 (2)	S(7)-Re(2)-S(3)	92.3 (2)
S(2)-Re(1)-S(4)	88.4 (3)	S(7)-Re(2)-S(4)	86.9 (3)
S(2)-Re(1)-S(5)	153.9 (3)	S(7)-Re(2)-S(5)	155.3 (3)
S(2)-Re(1)-N(1)	99.7 (7)	S(7)-Re(2)-N(3)	97.9 (6)
S(3)-Re(1)-S(4)	73.2 (2)	S(3)-Re(2)-S(4)	73.6 (2)
S(3)-Re(1)-S(5)	75.3 (2)	S(3)-Re(2)-S(5)	75.5 (2)
S(3)-Re(1)-N(1)	164.0 (7)	S(3)-Re(2)-N(3)	163.3 (6)
S(4)-Re(1)-S(5)	109.7 (3)	S(4)-Re(2)-S(5)	109.4 (3)
S(4)-Re(1)-N(1)	96.8 (6)	S(4)-Re(2)-N(3)	93.7 (6)
S(5)-Re(1)-N(1)	96.7 (6)	S(5)-Re(2)-N(3)	99.4 (6)
Re(1)-N(1)-N(2)	171.4 (19)	Re(2)-N(3)-N(4)	170.0 (18)
Re(1)-S(1)-C(11)	111.5 (10)	Re(2)-S(6)-C(61)	111.1 (12)
Re(1)-S(2)-C(21)	113.9 (10)	Re(2)-S(7)-C(71)	115.6 (10)
Re(1)-S(3)-C(31)	110.3 (9)	Re(2)-S(3)-C(31)	120.9 (9)
Re(1)-S(4)-C(41)	114.0 (8)	Re(2)-S(4)-C(41)	112.9 (9)
Re(1)-S(5)-C(51)	117.1 (9)	Re(2)-S(5)-C(51)	115.9 (9)
Re(1)-S(3)-Re(2)	65.7 (1)		
Re(1)-S(4)-Re(2)	70.8 (1)		
Re(1)-S(5)-Re(2)	70.8 (2)		

geometries exhibiting extensive multiple bonding.³¹

Although the structure of **3a** shares common features with the general class of triply bridged binuclear complexes listed in Table IX, the detailed geometry represents a unique structural type. The complex monoanion is binuclear with equivalent pseudooctahedral molybdenum centers sharing a common face defined by the three bridging thiolate donors. The coordination about each molybdenum atom is completed by the thiolate sulfur atoms of the terminally coordinated thiophenolate groups and by the σ -nitrogen atoms of the diazenido ligands. The Mo-S distances to the bridging thiolate ligands trans to the diazenido groups are significantly longer than the average of all other Mo-S distances (2.59 (6) vs. 2.507 (6) Å).

An unusual feature of this structure is the presence of two σ -diazenido ligands on each Mo center. If we consider each diazenido ligand to contribute three electrons, the Mo centers attain an 18-electron count without the necessity of a metal-metal bond. As a consequence, the Mo-Mo distance is 3.528 (1) Å, significantly longer than any other metal-metal distance reported in Table VIII and consistent with the absence of a metal-metal bond. The bridge symmetry approximations C_{3v} , rather than the C_{2v} symmetry associated with all other members of this class. Concomitant to the lengthening of the Mo-Mo distance is a significant expansion of the valence angles at the bridging thiolates and a lengthening of the Mo-S bridging distances. The $\beta = 70.53$ parameter gives values of 14.5, 16.2, and 17.9°, consistent with the absence of a metal-metal bond.

The structures of **2** and **3a** illustrate the remarkable ability of the diazenido grouping to stabilize a variety of metal-thiolate geometries and to allow unusual coordination types by virtue of its function as a three-electron donor. The consequences of introducing a second π -bonding diazenido unit on each metal center in **3a** on the bonding are illustrated schematically in Figure 4, which contrasts simple bonding schemes for structures of type **2** with that derived for **3a**. Whereas the 34-electron structures of type **2** have available d_{xy} -type orbitals on each metal to generate metal-metal bonding and antibonding orbitals, the 36-electron structures must utilize all the metal t_{2g} -type orbitals in π -bonding to the organodiazenido groups. Any electron density that had been available for metal-metal bonding in type **2** structures is now drained away into π -bonding to the NNPh groups. Alternatively, the view may be taken that the $a_2 \sigma^*$ orbital of type **2** structures is stabilized in **3** by interaction with the organodiazenido π^* orbitals and hence may accommodate an additional two electrons, giving rise to the electron-precise structure with no net metal-metal interaction.

Conclusions. The structures **2**, **3a**, and **4** illustrate the remarkable flexibility of the triply bridged binuclear core when the pseudoapical ligand is the organodiazenido functionality. Thus, **2** and **4** display the common C_{2v} symmetry type with a short metal-metal distance, while **3a** adopts a unique approximately C_{3v} bridge geometry with a long nonbonding metal-metal distance. Metal-metal distances in the range of 2.63-3.53 Å have now been reported for triply bridged binuclear complexes of this class. The diazenido grouping also appears to facilitate trans thiolato coordination and consequently favor a triple thiolato bridge geometry. Furthermore, the persistence of the *cis*-bis(diazenido)molybdenum core confirms the robust chemical nature of this unit and suggests a continuing evolution of its coordination geometry. Unlike the

Table IX. Comparison of Selected Parameters for Triply Bridged Binuclear Complexes of Molybdenum, Tungsten, and Rhenium

complex	distances, Å				angles, deg						Mo ₂ XY dihedral	Mo displacement, %	ref
	Mo-Mo	Mo-X	Mo-Y	Mo-Z	Mo-X-Mo	Mo-Y-Mo	Mo-Z-Mo	X-Mo-Y	X-Mo-Z	Y-Mo-Z			
$[\text{Mo}_2\text{O}_2(\text{OMe})_2(\text{SC}_6\text{H}_4\text{Me-4})_6]^-$	2.919 (5)	2.47 (2) [SR]	2.47 (2) [SR]	2.11 (2) [OR]	72.6 (5)	72.6 (5)	87.6 (6)	106.5 (3)	69.5 (8)	69.5 (8)	174.3	0.42 (1)	1
$[\text{Mo}_2\text{O}_2\text{S}(\text{SCH}_2\text{CH}_2\text{O})_2(\text{S}_2\text{CNEt}_2)_2]^-$	2.725 (1)	2.489 (3) [SR]	2.334 (1) [S ²⁻]	2.202 (14) [OR]	66.4 (4)	71.4 (4)	76.5 (9)	110.4 (5)	68.0 (1)	77.9 (2)	164.6	0.39	2
$[\text{Mo}_2\text{O}_2(\text{SCH}_2\text{CH}_2\text{O})_2(\text{oxinate})_2]^-$	2.628 (1)	2.484 (2) [SR]	1.937 (12) [O ²⁻]	2.190 (17) [OR]	63.9 (6)	85.5 (2)	75.8 (7)	104.5 (2)	70.4 (2)	74.6 (4)	164.1	0.39	3
$[\text{Mo}_2\text{O}_2(\text{SCH}_2\text{CH}_2\text{O})_2]^{2-}$	2.676 (1)	2.506 (16) [SR]	1.957 (12) [O ²⁻]	2.215 (15) [OR]	64.5 (1)	86.3 (2)	74.3 (2)	104.0 (8)		73.6 (3)	167.0	0.39	4
$[\text{Mo}_2\text{O}_2(\text{SPh})_2(\text{S}_2\text{CNEt}_2)_2]^-$	2.677 (5)	2.49 (7) [SR]	2.045 (31) [O ²⁻]	2.688 (11) [SR]	65.0 (5)	81.8 (16)	59.7 (9)	106.6 (9)	70.8 (2)	73.6 (3)	178.0	0.39	5
$[\text{Mo}_2\text{O}_2(\text{SPh})_2\text{Cl}(\text{SCN}(\text{Et}_2)_2)]^+$	2.822 (2)	2.455 (4) [SR]	2.460 (8) [SR]	2.613 (12) [Cl]	70.2 (1)	70.7 (1)	63.4 (1)	109.9 (1)	73.1 (3)	71.9 (1)	177.7	0.40	6
$[\text{Mo}_2\text{O}_2(\text{SCH}_2\text{CH}_2\text{O})_2\text{Cl}]^-$	2.728 (1)	2.480 (12) [SR]	2.014 (17) [OR]	2.176 (39) [OR]	66.7 (1)	85.2 (1)	77.6 (1)	103.0 (2)	69.5 (9)	73.3 (6)	163.4	0.30	7
$[\text{Mo}_2\text{O}_2(\text{SCH}_2\text{CH}_2\text{O})_2\text{Cl}]^-$	2.731 (1)	2.480 (21) [SR]	2.024 (12) [OR]	2.176 (27) [OR]	66.8 (1)	84.9 (3)	77.7 (3)	103.2 (7)	69.6 (3)	73.0 (8)	164.6	0.33	7
$[\text{Mo}_2\text{O}_2(\text{SCH}_2\text{CH}_2\text{O})_2(\text{SCH}_2\text{CH}_2\text{OH})]^-$	2.739 (1)	2.483 (18) [SR]	2.055 (5) [OR]	2.194 (30) [OR]	67.0 (1)	83.6 (1)	77.2 (1)	104.3 (8)	69.2 (9)	71.6 (7)	168.5	0.38	7
$[\text{Mo}_2\text{O}_2\text{Cl}_2(\text{SPh})_2]^-$	2.915 (1)	2.445 (3) [SR]	2.449 (3) [SR]	2.651 (3) [Cl]	73.2 (1)	73.0 (1)	66.7 (1)	106.9 (1)	72.2 (1)	74.3 (1)	172.5	0.40	8
$[\text{Mo}_2\text{O}_2(\text{SPh})_2(\text{S}_2\text{CNEt}_2)_2]^-$	2.649 (1)	1.957 (7) [O ²⁻]	2.474 (4) [SR]	2.644 (3) [SR]	85.4 (4)	64.7 (1)	59.6 (1)	104.9 (3)	70.7 (2)	72.1 (1)	170.9	0.40	8
$[\text{Mo}_2(\text{NNPh})(\text{NNHPh})(\text{SCH}_2\text{CH}_2\text{S})_3(\text{SCH}_2\text{CH}_2\text{SH})]^-$	2.837 (2)	2.424 (6) [SR]	2.431 (6) [SR]	2.577 (6) [SR]	71.0 (1)	71.7 (1)	66.9 (1)	108.6 (1)	72.2 (1)	74.3 (1)	172.7	0.45	13, b
$[\text{Mo}_2(\text{NNPh})_2(\text{SPh})_4(\text{SPh})_4]^-$	3.527 (1)	2.570 (6) [SR]	2.644 (6) [SR]	2.487 (6) [SR]	86.7 (1)	83.7 (1)	87.9 (2)	87.0 (2)	72.9 (2)	73.9 (2)			15, b
$[\text{W}_2\text{O}_2\text{Cl}_2(\text{SC}_6\text{H}_4)_2]^-$	2.854 (2)	2.414 (8) [SR]	2.421 (7) [SR]	2.635 (6) [Cl]	72.2 (2)	72.4 (2)	66.0 (2)	105.5 (3)	77.7 (2)	78.2 (2)	164.4	0.26	10
$[\text{W}_2\text{O}_2\text{Cl}_2(\text{SPh})_2]^-$	2.8824 (7)	2.436 (2) [SR]	2.455 (3) [SR]	2.596 (3) [Cl]	72.5 (1)	72.0 (1)	67.3 (1)	107.6 (1)	77.8 (1)	72.1 (1)	175.9	0.38	11
$[\text{W}_2\text{O}_2\text{Cl}_2(\text{SC}_6\text{H}_4\text{Me})_2]^-$	2.878 (2)	2.450 (7) [SR]	2.467 (8) [SR]	2.604 (7) [Cl]	72.3 (2)	72.3 (2)	67.1 (2)	107.6 (2)	71.9 (2)	75.2 (2)	176.7	0.39	11
$[\text{Re}_2(\text{SPh})(\text{NO})_2]^-$	2.783 (1)	2.385 (1) [SR]	2.408 (5) [SR]	2.553 (5) [SR]	70.8 (2)	70.9 (2)	65.7 (1)	109.3 (2)	71.5 (2)	75.2 (2)	178.1		12
$[\text{Re}_2(\text{SPh})_2(\text{NNPh})_2]^-$	2.747 (2)	2.382 (7) [SR]	2.401 (7) [SR]	2.548 (7) [SR]	70.4 (2)	65.6 (2)	69.8 (2)	109.7 (3)	73.7 (3)	75.3 (2)	176.4	0.40	14, b

^a Identity of X, Y, and Z noted in brackets. ^b This work.

well-developed $[\text{MoO}_2]^{2+}$ unit, the $[\text{Mo}(\text{NNR})_2]^{2+}$ moiety may also undergo considerable chemistry of its own, such as protonation, alkylation, and N-N bond cleavage.

Acknowledgment. This work was supported in part by a grant from the National Science Foundation (CHE8514634) to J.Z. We thank Peter Bishop of the University of Essex for assistance

with the electrochemical studies.

Supplementary Material Available: Tables reporting bond lengths, bond angles, anisotropic temperature factors, and calculated hydrogen atom positions and thermal factors for **2**, **3a**, and **4** (33 pages); tables giving observed and calculated structure factors for **2**, **3a**, and **4** (155 pages). Ordering information is given on any current masthead page.

Contribution from the Departments of Chemistry, University of Hong Kong, Pokfulam Road, Hong Kong, and The Chinese University of Hong Kong, Shatin, New Territories, Hong Kong

Synthesis and Reactivities of *trans*-Dioxoosmium(VI) Schiff-Base Complexes. X-ray Crystal Structure of Dioxo[*N,N'*-(1,1,2,2-tetramethylethylene)bis(3-*tert*-butylsalicylideneaminato)]osmium(VI)

Chi-Ming Che,*^{1a} Wing-Kin Cheng,^{1a} and Thomas C. W. Mak*^{1b}

Received June 1, 1987

The syntheses and redox properties of *trans*-dioxoosmium(VI) Schiff-base complexes are described. The crystal structure of *trans*-[Os^{VI}O₂(3-*t*-Bu-saltmen)] has been determined: C₂₈H₃₈N₂O₄Os, space group *P*₂₁/*c*, *a* = 11.918 (6) Å, *b* = 10.416 (1) Å, *c* = 23.53 (1) Å, β = 102.91 (3)°, *Z* = 4, *R* = 0.062 for 3651 observed Mo Kα data. The measured osmyl Os-O bond distances are 1.722 (8) and 1.760 (7) Å; other than this, the molecule conforms well to idealized C₂ symmetry. Both electrochemical oxidation and reduction of *trans*-dioxoosmium(VI) Schiff-base complexes are irreversible in acetonitrile.

Introduction

There is a growing interest in the oxidation chemistry of ruthenium and osmium complexes containing multianionic chelating ligands.^{2,3} Recent studies by Groves and co-workers³ showed that the dioxoruthenium(VI) porphyrin complex [RuO₂(TMP)] (TMP = tetramethylsitylporphyrinato dianion) is an excellent catalyst for aerobic epoxidation of alkenes. We have been intrigued by this work and suspect that similar reaction chemistry of ruthenium complexes may also be observed by using inexpensive Schiff-base ligands, such as salen [*N,N'*-ethylenebis(salicylideneaminato)]. In an attempt to develop the chemistry of high-valent ruthenium-salen-oxo complexes, we believe that knowledge of the physical and redox properties of the analogous osmium complexes, which are less reactive but more stable than the ruthenium system, is important. The synthesis of [Os^{VI}O₂(salen)] and X-ray structure of [Os^{IV}(salen)(SPh)₂] have previously been reported.⁴ However, the [Os^{IV}O₂(salen)] complex is virtually insoluble in common organic solvents, rendering the study of its solution chemistry difficult. In this contribution, we describe the preparation and spectroscopic and redox properties of five *trans*-dioxoosmium(VI) complexes containing different kinds of Schiff-base ligands. The osmyl Os-O bond distances in *trans*-[Os^{VI}O₂(3-*t*-Bu-saltmen)] [3-*t*-Bu-saltmen = *N,N'*-(1,1,2,2-tetramethylethylene)bis(3-*tert*-butylsalicylideneaminato)] (Figure 1), as determined by X-ray crystallography, are 1.760 (7) and 1.722 (8) Å.

Experimental Section

The Schiff-base ligands (Figure 1) were prepared by the literature methods.⁵ All other reagents used were of analytical grade.

***trans*-[Os^{VI}O₂(5-*i*-Pr-salen)] (1).** K₂[OsO₂(OH)₄] (0.50 g) and 5-*i*-Pr-salenH₂ (0.45 g) were stirred in methanol (150 mL) for 30 min. An orange-red solid gradually precipitated upon standing. This was filtered

Table I. Microanalytical Data for the Osmium Complexes

complex	found (calcd)		
	% C	% H	% N
1	46.50 (46.14)	4.80 (4.54)	5.10 (4.89)
2	48.73 (48.98)	5.30 (5.10)	4.45 (4.67)
3	51.11 (51.12)	5.98 (5.79)	4.07 (4.27)
4	52.68 (52.63)	6.05 (6.14)	4.11 (4.09)
5	48.39 (48.59)	5.66 (6.14)	3.73 (3.44)

Table II. UV-Vis Spectral Data for the Osmium Complexes in CH₂Cl₂

complex	λ _{max} , nm (log ε)
1	410 (3.88), 367 (4.08), 290 (4.48), 267 (4.50), 243 (4.92), 228 (4.84)
2	405 (3.81), 367 (3.99), 293 (4.55), 267 (4.56), 245 (4.94), 238 (4.91)
3	420 (3.72), 368 (3.99), 310 (4.41), 265 (4.50), 245 (4.86), 233 (4.84)
4	408 (3.89), 369 (4.02), 305 (4.43), 267 (4.51), 243 (4.98), 231 (4.84)
5	415 (3.92), 368 (4.17), 302 (4.55), 268 (4.56), 243 (4.99), 230 (4.85)

off, washed with a methanol/diethyl ether mixture (1:10), and dried under vacuum at room temperature (yield ~65%). Pure samples of **1** were obtained by slow diffusion of diethyl ether into a dichloromethane solution of the crude product. IR (Nujol mull): ν_{as}(Os=O) 845 cm⁻¹.

The following complexes were similarly prepared as described for **1**: *trans*-[Os^{VI}O₂(5-*t*-Bu-salen)] (**2**), *trans*-[Os^{VI}O₂(3-*t*-Bu-saltmen)] (**3**), *trans*-[Os^{VI}O₂(5-(3-Me)-Bu-saltmen)] (**4**), and *trans*-[Os^{VI}O₂(5-*t*-Bu-saltmen)] (**5**).

Physical Measurements. ¹H NMR spectra were obtained on a Jeol FX-90Q Fourier transform spectrometer. Cyclic voltammetric measurements were performed by using a PAR universal programmer (Model 175), potentiostat (Model 173), and digital coulometer (Model 179). Formal potential measurements were made against a Ag/AgNO₃ (0.1 M in CH₃CN) electrode with ferrocene as the internal standard and pyrolytic graphite as the working electrode. Acetonitrile for electrochemical studies was distilled over CaH₂. The supporting electrolyte was [Bu₄N]PF₆. Microanalytical data for the newly prepared complexes are tabulated in Table I. The UV-vis spectral data and ¹H NMR and electrochemical data of complexes **1-5** are tabulated in Tables II-IV, respectively.

- (1) (a) University of Hong Kong. (b) The Chinese University of Hong Kong.
 (2) See for example: (a) Che, C. M.; Cheng, W. K.; Leung, W. H.; Mak, T. C. W. *J. Chem. Soc., Chem. Commun.* **1987**, 418. (b) Anson, F. C.; Collins, T. J.; Gipson, S. L.; Keech, J. T.; Krafft, T. E.; Peake, G. T. *J. Am. Chem. Soc.* **1986**, *108*, 6593. (c) Anson, F. C.; Christie, J. A.; Collins, T. J.; Coots, R. J.; Furutani, T. T.; Gipson, S. L.; Keech, J. T.; Krafft, T. E.; Santarsiero, B. D.; Spies, G. H. *J. Am. Chem. Soc.* **1984**, *106*, 4460. (d) Che, C. M.; Cheng, W. K.; Mak, T. C. W. *J. Chem. Soc., Chem. Commun.* **1986**, 200. (e) Che, C. M.; Chung, W. C. *J. Chem. Soc., Chem. Commun.* **1986**, 386. (f) Leung, T.; James, B. R.; Dolphin, D. *Inorg. Chim. Acta* **1983**, *79*, 180.
 (3) Groves, J. T.; Quinn, R. *J. Am. Chem. Soc.* **1985**, *107*, 5790.
 (4) Che, C. M.; Cheng, W. K.; Mak, T. C. W. *Inorg. Chem.* **1986**, *25*, 703.
 (5) Gall, R. S.; Rogers, J. F.; Schaefer, W. P.; Christoph, G. G. *J. Am. Chem. Soc.* **1976**, *98*, 5135.